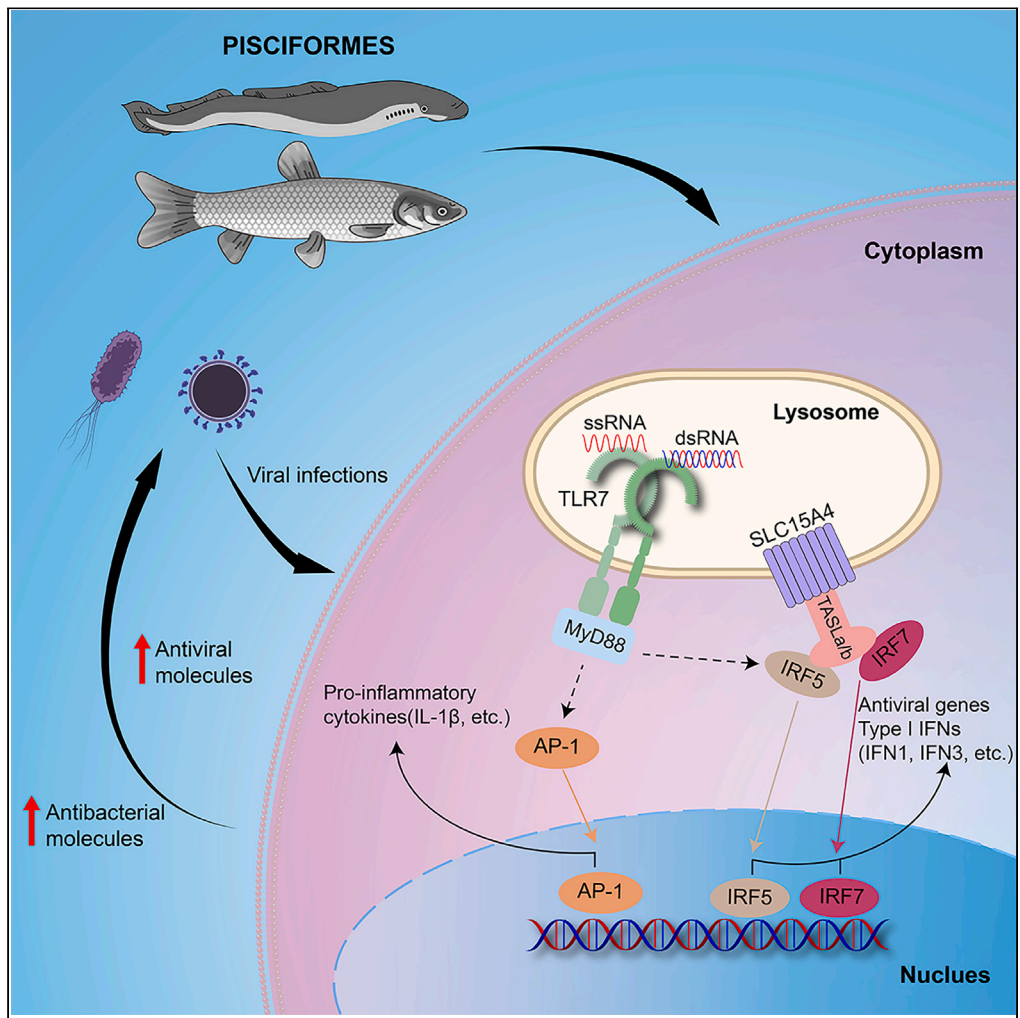**Article**

TLR7 neo-functionalizes to sense dsRNA and trigger antiviral and antibacterial immunity in non-tetrapod vertebrates

Rui Jiang, Wentao Zhu, Zhiwei Liao, Chunrong Yang, Jianguo Su

sujianguo@mail.hzau.edu.cn

Highlights

TLR7 senses both ssRNA and dsRNA and triggers immune responses in pisciformes

TLR7 induces IFN response via SLC15A4/TASLa/ TASLb/IRF5/IRF7 complex in teleost

TLR7 boosts pro-inflammatory cytokines via AP-1, not NF-κB pathway in teleost

Article

TLR7 neo-functionalizes to sense dsRNA and trigger antiviral and antibacterial immunity in non-tetrapod vertebrates

Rui Jiang,[1,2] Wentao Zhu,[1] Zhiwei Liao,[1] Chunrong Yang,[3] and Jianguo Su[1,2,4,*]

SUMMARY

TLR7 plays a crucial role in sensing viral ssRNA and initiating immune responses. Piscine TLR7 also responds to dsRNA challenge. dsRNA exists in almost all the viruses at specific stages. However, the mechanism on sensing dsRNA by TLR7 remains unknown. In the present study, we employed *Ctenopharyngodon idella* TLR7 (CiTLR7) to systematically explore the immune functions and mechanisms in teleost. CiTLR7 can directly bind not only ssRNA but also dsRNA at different patches in lysosome, recruit MyD88 as adaptor, and activate the downstream IFN pathway via SLC15A4/TASLa/TASLb/IRF5/IRF7 complex for antiviral and antibacterial infections and AP-1 pathway for pro-inflammatory cytokines. The key binding sites for dsRNA are L29 and L811 in CiTLR7. Further, we found that the function on recognizing dsRNA by TLR7 emerges in pisciformes and loses in tetrapods in evolution. This is the first report on sensing both ssRNA and dsRNA by a TLR member.

INTRODUCTION

Toll-like receptors (TLRs) play critical roles in both the innate immune system and adaptive immune system by recognizing microbe- or danger-associated molecular patterns (MAMPs or DAMPs).[1–3] These MAMPs range from bacterial cell surface components to viral genomes, including lipopolysaccharide (LPS), peptidoglycan (PGN), lipoteichoic acid, mannan, glucan, and nucleic acid.[1,4] TLR comprises a leucine-rich repeat (LRR)-containing ectodomain, a single transmembrane (TM) domain, and an intracellular toll/interleukin-1 receptor (TIR) domain. The ectodomain recognizes a wide variety of MAMPs, whereas the cytoplasmatic TIR domain engages in downstream signal transduction.[5] Upon stimulation with MAMPs, TLRs initiate signal transduction pathways via one or more following adaptors: myeloid differentiation primary response 88 (MyD88), TIR-domain-containing adaptor-inducing interferon-β (IFN-β) (TRIF), TIR-domain-containing adaptor protein (TIRAP), TRIF-related adaptor molecule (TRAM), sterile-α and armadillo-motif-containing protein 1 (SARM1), B cell adapter for phosphoinositide 3-kinase (BCAP), and SLP adaptor and C-terminal Src kinase (CSK)-interacting membrane protein (SCIMP).[6] TRAM is absent in teleost genomes.[7] SARM1 and BCAP are negative adaptors in TLR signaling.[7] SCIMP is a transmembrane non-TIR-containing adaptor, binding directly to the TLR4-TIR domain in response to LPS.[6] Subsequently, a wide range of transcriptional factors are activated, such as IFN regulatory factors (IRFs), nuclear factor κB (NF-κB), and adaptor protein complex-1 (AP-1), leading to productions of IFNs, inflammatory cytokines, chemokines, antimicrobial peptides, etc. These molecules cause activation of macrophages, recruitment of neutrophils, and induction of IFN-stimulated genes, leading to direct killing of the invading pathogens and activating adaptive immunity.[1]

TLR family members are different in various animals, such as TLR1-10 in humans (*Homo sapiens*), TLR1-9 and TLR11-13 in mouse (*Mus musculus*), and 21 members in grass carp (*Ctenopharyngodon idella*).[8] TLR3, 5, 7–10, 13, 19, 21, and 22 can sense microbial nucleic acids: TLR3, 5, 10, 19, and 22 for viral double-stranded RNA (dsRNA); TLR7 and 8 for viral single-stranded RNA (ssRNA); TLR9 and 21 for viral and bacterial CpG-ODN; and TLR13 for bacterial rRNA, respectively.[1,5,9–15] TLR7 recognizes viral ssRNA in lysosome,[16–18] recruits MyD88 as adaptor,[19] and induces productions of type I IFN and inflammatory cytokines.[20] DsRNA, as a pivotal viral MAMP, not only exists in dsRNA viruses but also generates during viral infection as a replication intermediate for ssRNA viruses or as a by-product of symmetrical transcription in DNA viruses.[21,22] dsRNA in cell surface or endosome formed by endocytosing viruses is recognized by TLR3, recruiting TRIF as adaptor in mammals.[23] Then, TRIF undergoes oligomerization and recruits a signaling complex involving TANK-binding kinase 1 (TBK1) and atypical inhibitor of κB kinase ε (IKKε) via tumor-necrosis-factor (TNF)-receptor-associated factor 3 (TRAF3) for IRF3 and IRF7 phosphorylation and activation,[24] consequently inducing type I IFNs.[25,26] Type I IFNs play crucial role in antiviral immunity and contain IFN1-4 members in zebrafish (*Danio rerio*) and grass carp.[27] IRF5 is also critical for antiviral immunity.[28] Meanwhile, TRIF also recruits TRAF6 and activates TGF-β-activated kinase 1 (TAK1) for NF-κB activation and interleukin-1β (IL-1β) production.[29] The classical NF-κB signaling pathway plays a crucial role in innate

immunity, and its activation could induce proinflammatory cytokines in response to infection or injury.[30] Another dsRNA sensor is TLR10 in human, which predominantly localizes to endosomes and recruits MyD88 as adaptor and suppresses IRF7-dependent type I IFN production. TLR10 competes with TLR3 for dsRNA binding and inhibits TLR3 signaling in response to dsRNA stimulation.[10] Recently, more TLRs have been identified to recognize dsRNA in poikilotherms, such as TLR5a/b in Cyprinids,[5] TLR19 in teleost,[12] and TLR22a/b in ectothermic vertebrates.[14]

Solute carrier family 15 member 4 (SLC15A4) is an endolysosome-resident amino acid transporter that is crucial for trafficking and colocalization of nucleic-acid-sensing TLRs and their ligands to endolysosomes.[31] TLR adaptor interacting with SLC15A4 on the lysosome (TASL) contains a conserved pLxIS motif (in which p denotes a hydrophilic residue and x denotes any residue) that mediates the recruitment and activation of IRF5 and whose localization and function rely on the interaction with SLC15A4.[18] TASL is necessary for TLR7, TLR8, and TLR9 signaling in mammals.[18]

In the present study, we employed grass carp, the worldwide top-yield economic fish, to investigate the subcellular localization, ligands and binding sites, adaptor, signaling pathways, and immune functions of TLR7 in teleosts. We found that CiTLR7 senses not only ssRNA but also dsRNA in lysosome, recruits MyD88 as adaptor, and exerts antiviral role in not only ssRNA virus (spring viraemia of carp virus, SVCV) but also dsRNA virus (grass carp reovirus, GCRV) infections and also antibacterial function mediated by IFN1 and AP-1. Further, the immune signaling pathways are different in between teleosts and mammals. Furthermore, we demonstrated that the characterization of binding dsRNA for TLR7 exists in pisciformes but not tetrapods. These results suggested that TLR7 in pisciformes exhibits neo-functionalization to sense dsRNA in evolution.

RESULTS

CiTLR7 recognizes not only ssRNA but also dsRNA

TLR7 senses ssRNA and activates antiviral immunity in mammals,[19] but the exact ligand of TLR7 remains unknown in teleost. Firstly, we employed five representative MAMPs (LPS, PGN, bacterial dsDNA, R848 [resiquimod, a ssRNA analogue], and poly(I:C) [polyinosinic-polycytidylic acid, a dsRNA analogue]) and two representative viruses (SVCV [a ssRNA virus] and GCRV [a dsRNA virus]) to stimulate *Ctenopharyngodon idella* kidney (CIK) cell line, respectively, and mRNA expressions of *CiTLR7* were examined by real-time quantitative RT-PCR (qRT-PCR). As shown in Figure 1A, mRNA expressions of *CiTLR7* were remarkably upregulated after R848, poly(I:C), SVCV, or GCRV stimulation, implying that CiTLR7 responds to ssRNA (R848 and SVCV) and dsRNA (poly(I:C) and GCRV). Then, dual-luciferase reporter (DLR) assay was performed to verify the results, which showed that R848 and poly(I:C) can activate IFN1, a representative antiviral and antibacterial type I IFN member in grass carp, whereas LPS, PGN, and dsDNA cannot (Figure 1B). Further, to provide the direct evidence for ligand binding, recombinant CiTLR7 ectodomain with GST-tag was expressed in *Escherichia coli*, purified and detected by sodium dodecyl sulfate-polyacrylamide gel electrophoresis (SDS-PAGE) and immunoblotting (IB) (Figure 1C); afterward, the binding abilities between recombinant ectodomain and ssRNA or dsRNA were examined by pull-down assay using biotin-ssRNA or biotin-poly(I:C) as bait at pH 7.4 and pH 5.5 (Figures 1D and 1E). To our surprise, the interaction was just observed between CiTLR7 ectodomain and biotin-ssRNA at pH 5.5 and pH 7.4 (Figure 1D), but not biotin-poly(I:C) (Figure 1E). Considering the structural change of CiTLR7 ectodomain expressed in prokaryote may affect protein function, eukaryotic fathead minnow (FHM) cells overexpressed CiTLR7-Myc and were used for pull-down assays (Figures 1F and 1G). The results demonstrated that CiTLR7 can bind not only ssRNA but also dsRNA in acidic compartment in piscine cells. Furthermore, we found the functional activation of CiTLR7 by ssRNA or dsRNA in dose-dependent manner and synergistic effect (Figure 1H). The results indicated that both ssRNA and dsRNA can bind CiTLR7 in acidic condition and synergistically activate IFN response.

CiTLR7 inhibits the proliferation of both ssRNA and dsRNA viruses

CiTLR7 can sense ssRNA and dsRNA, and trigger IFN response, which indicates CiTLR7 possesses the antiviral function. We employed SVCV and GCRV to testify the antiviral function of CiTLR7. Firstly, we overexpressed CiTLR7 in CIK and FHM cells and examined them by IB (Figure 2A). Then, standard plaque assay indicated that CiTLR7 overexpression inhibits GCRV-induced CIK cell death and SVCV-induced FHM cell death (Figure 2B). Next, we examined the influence of CiTLR7 on GCRV and SVCV titer. The results showed that GCRV and SVCV titers significantly decrease in CiTLR7 overexpression cells (Figures 2C and 2D). Further, we examined the influence of CiTLR7 on virus proliferation; the results showed that CiTLR7 overexpression inhibits virus gene transcription (GCRV-VP4, GCRV-VP56, SVCV-N, and SVCV-P) (Figures 2E and 2F). Furthermore, we verified the results by RNA interference. Among three candidate small interfering RNA (siRNA) sequences for CiTLR7, S1 showed the highest interference efficiency (Figure 2G) and was used as a representative siRNA for subsequent experiments. After that, we performed the plaque (Figure 2H), virus titer (Figure 2I), and virus gene transcription (Figure 2J) assays post-CiTLR7 knockdown. In addition, we also found that CiTLR7 can resist bacterial proliferation post-poly(I:C) stimulation (Figures 2E and 2F). The results consistently showed that CiTLR7 can inhibit the viral and bacterial proliferation.

CiTLR7-L29 and CiTLR7-L811 are key binding sites for dsRNA

CiTLR7 senses viral RNA, activates antiviral immunity, and thus protects cells from viral infections. What are the key sites for ligand binding and antiviral function in CiTLR7? Firstly, we predicted and modeled the binding sites for dsRNA and ssRNA by AlphaFold2, AutoDock Vina, and PyMOL software. The results showed that poly(I:C) successfully docks at the CiTLR7-ectodomain model (Figure 3A). CiTLR7 contains six predicted binding sites for poly(I:C) in AutoDock Vina simulation. All the six predicted binding sites were mutated into alanine, then the mutants were transfected into FHM cells to investigate the influence of the mutation on IFN1 promoter activity. The results indicated that CiTLR7-L29A
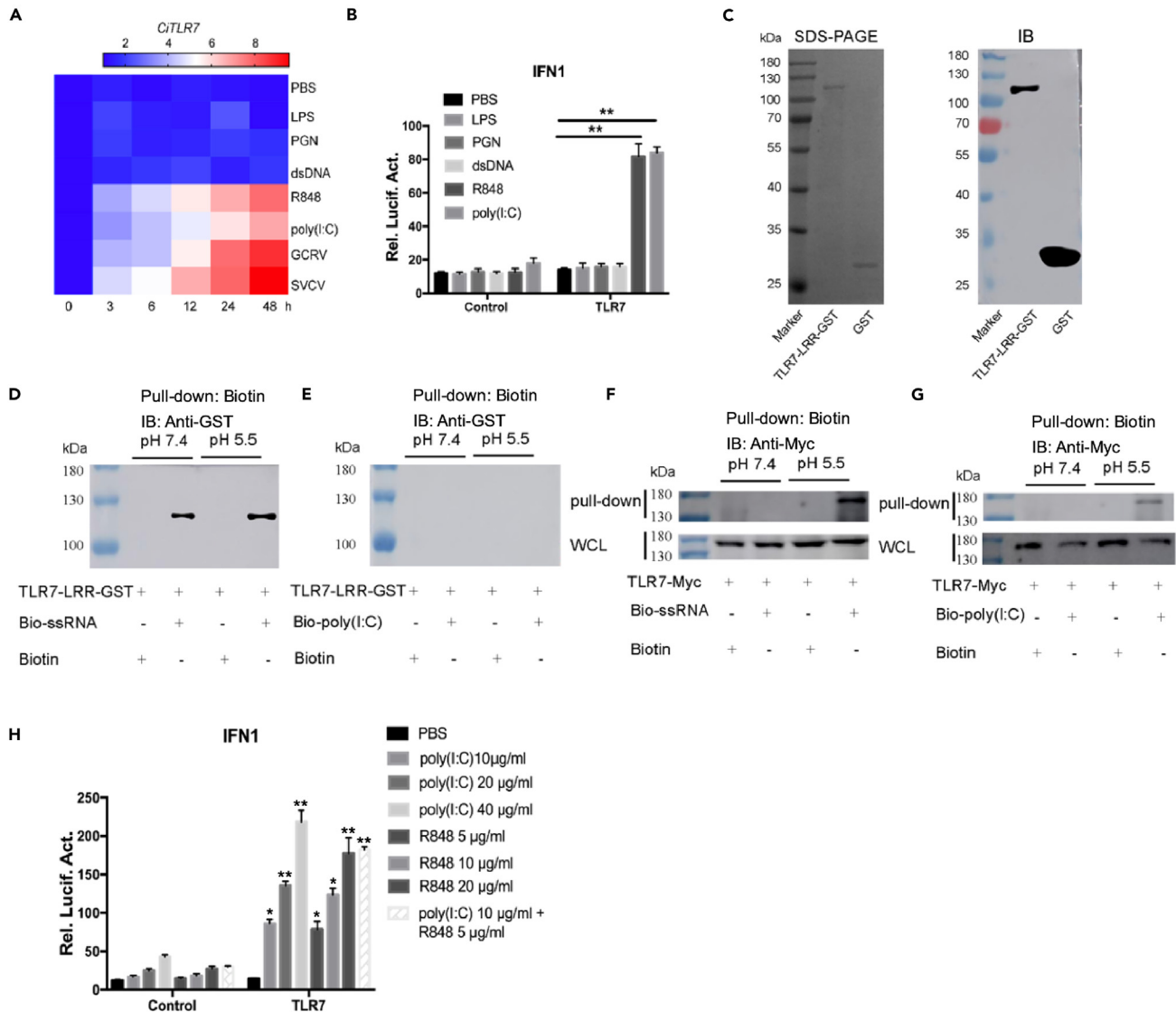
Figure 1. CiTLR7 recognizes ssRNA and dsRNA

(A) CIK cells were seeded in 12-well plate for 24 h, stimulated with PBS, LPS, PGN, bacterial dsDNA, R848, poly(I:C), GCRV, or SVCV for different time points (0, 3, 6, 12, 24, 48 h), and then mRNA expression of *CiTLR7* was measured by qRT-PCR (n = 4).

(B) CIK cells were transfected with 380 ng pCiTLR7-Myc or empty vector, 380 ng pIFN1pro-Luc, and 38 ng pRL-TK for 24 h; cells were stimulated with PBS, LPS, PGN, bacterial dsDNA, R848, or poly(I:C) for 12 h. IFN1 promoter activity was measured by DLR assay (n = 3).

(C) Recombinant expression and purification of CiTLR7-ectodomain (GST-tag) protein was analyzed by SDS-PAGE (left) and IB (right); pGEX-4T-1 expression vector (GST-tag) protein was used as a control.

(D and E) CiTLR7-ectodomain protein was incubated with biotin-ssRNA (1 μg/mL), biotin-poly(I:C) (1 μg/mL), or biotin (control) at pH 7.4 or pH 5.5 for 1 h at 4°C; mixed with streptavidin agarose beads for 2 h at 4°C; and centrifuged, washed, denatured, and analyzed by IB with anti-GST Ab.

(F and G) Lysates of FHM cells overexpressing CiTLR7 were respectively incubated with biotin-ssRNA (1 μg/mL), biotin-poly(I:C) (1 μg/mL), or biotin (control, 1 μg/mL) at pH 7.4 or pH 5.5 for 1 h at 4°C; mixed with streptavidin agarose beads for 2 h at 4°C; and centrifuged, washed, denatured, and analyzed by IB with anti-Myc Ab.

(H) Effects of different concentrations of poly(I:C) and R848 on IFN1 promoter activity were measured by DLR assay in CIK cells (n = 3). **p < 0.01.

totally abolishes the increasement of promoter activity induced by poly(I:C), and CiTLR7-L811A significantly decreases IFN1 promoter activity compared with control; other mutants have no significant impact on IFN1 activity compared with control (Figure 3B). Further, pull-down and IB assays showed that the binding capacity for poly(I:C) is totally abrogated in CiTLR7-L29A and is obviously reduced in CiTLR7-L811A, whereas other mutants have no noticeable impact (Figure 3C). These results indicated that CiTLR7-L29 and CiTLR7-L811 are the key binding sites for dsRNA in CiTLR7. The binding sites for ssRNA have been addressed in human TLR7.[32] The predicted binding sites for ssRNA in CiTLR7 are
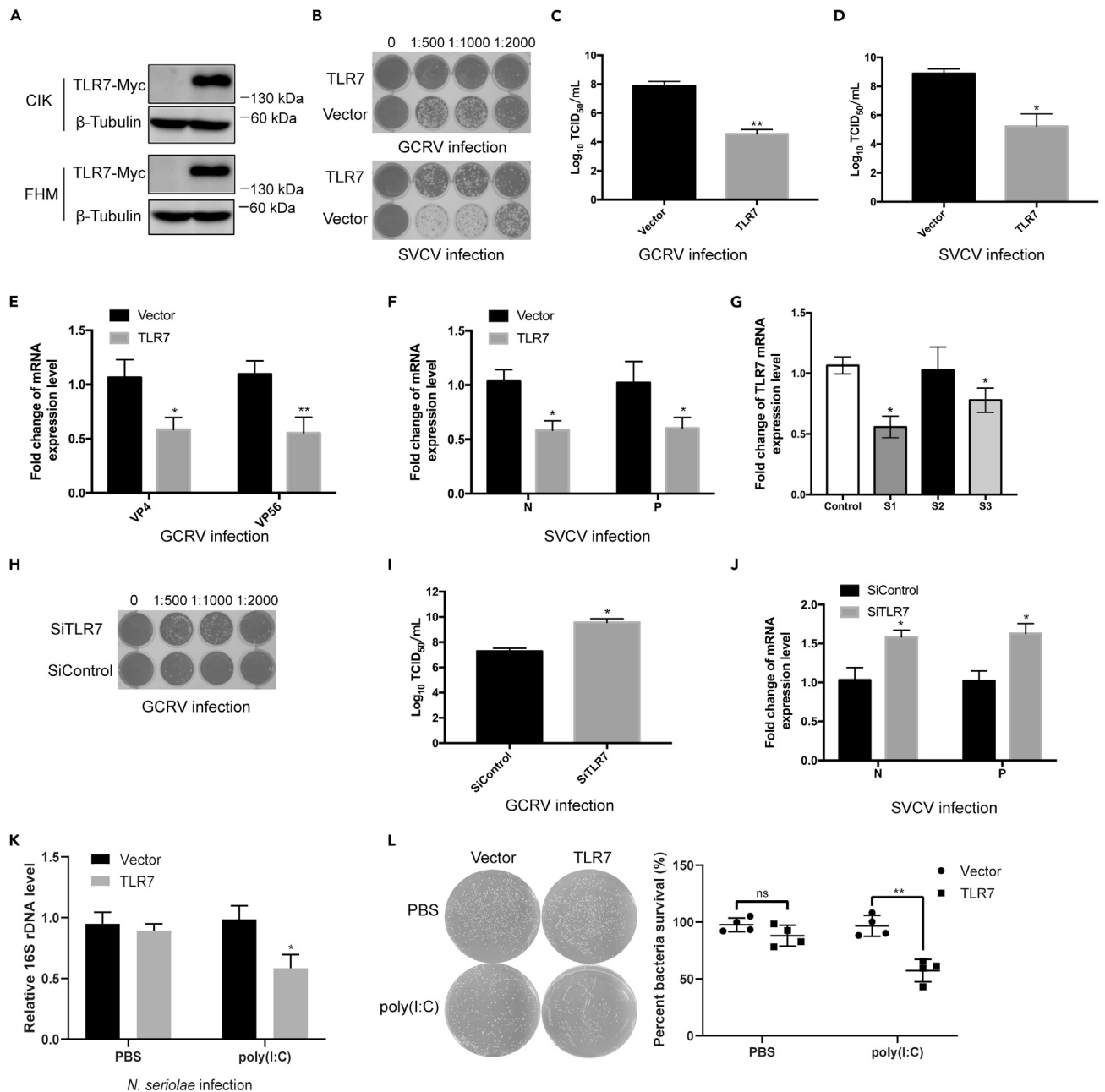
Figure 2. CiTLR7 protects CIK or FHM cells from viral and bacterial infections

(A) Efficiencies of CiTLR7 overexpression in CIK or FHM cells were respectively detected by IB with β-tubulin as the reference.

(B) Standard plaque assays in CIK or FHM cells overexpressing CiTLR7 or vector for 24 h and different dilutions of GCRV or SVCV infections for 48 h.

(C and D) CIK or FHM cells overexpressing constructs for 24 h were infected with GCRV or SVCV at an MOI = 0.1, and supernatants were collected at 24 h for viral titer assays by $TCID_{50}$ (n = 3).

(E) CIK cells overexpressing CiTLR7 were treated with supernatants for titer assays for 24 h, and mRNA expressions of GCRV *VP4* and *VP56* genes were measured by qRT-PCR (n = 4).

(F) FHM cells overexpressing CiTLR7 were treated with supernatants for titer assays for 24 h, and mRNA expressions of SVCV *N* and *P* genes were measured by qRT-PCR (n = 4).

(G) Interference efficiencies of siRNAs for CiTLR7 were detected by qRT-PCR.

(H) Standard plaque assay in CIK cells interfered with optimal siRNA (S1) for 12 h and different dilutions of GCRV infection for 48 h.

(I) CIK cells interfering CiTLR7 for 12 h were infected with GCRV at an MOI = 0.1, and supernatants were collected at 24 h for viral titer assays by $TCID_{50}$ (n = 3).

Figure 2. Continued

(J) CIK cells interfering CiTLR7 for 12 h were treated with supernatants for titer assays for 24 h, and mRNA expressions of GCRV *VP4* and *VP56* were measured by qRT-PCR (n = 4).

(K) CIK cells overexpressing constructs for 12 h and stimulated with poly(I:C) or PBS for 24 h were infected with *Nocardia seriolae* at 10^5 PFU/mL, and samples (cells and supernatants) were collected at 6 h for bacterial quantification, and 16S rDNA and EF1α were measured by qPCR (n = 4).

(L) The above samples were lysed, diluted, and plated for 7 days. The representative plates were shown (n = 4). *p < 0.05, **p < 0.01.

abundant (17 predicted binding sites) (Figure 3A). The binding sites of TLR7 for ssRNA are conserved between grass carp and human (Figure 3D). CiTLR7 binds dsRNA and ssRNA at different patches as a dual receptor.

CiTLR7 locates at lysosome and recruits MyD88 as adaptor

The subcellular localization has a critical impact on sensing ligands. To investigate the subcellular location of CiTLR7, we co-transfected plasmids CiTLR7-GFP (green fluorescent protein) and different organelle marker genes fusing RFP (red fluorescent protein) into CIK cells, respectively. The results showed that CiTLR7 colocalizes with LAMP2 (marker for lysosome), GRP78 (marker for endoplasmic reticulum [ER]), and GM130 (marker for Golgi apparatus), not RAB5 (marker for early endosome) and RAB7 (marker for late endosome) (Figures 4A and S1), which indicated that CiTLR7 locates at lysosome, ER, and Golgi apparatus. CiTLR7 is synthesized in ER and glycosylated in Golgi apparatus. Finally, CiTLR7 locates in lysosome (acidic compartment) to sense ligands ssRNA and dsRNA.

CiTLR7 recognizes ssRNA and dsRNA in lysosome. Further, what is the adaptor(s) of CiTLR7? Previous studies reported that the BB-loop of the TIR domain in TLRs interacts with adaptors.[33,34] All the human TLRs, except TLR3, have a conserved proline residue in the BB-loop, thought to bind MyD88. Thus, the partial amino acid sequences and crystal structures of TIR domain in CiTLR7, HsTLR7, CiTLR22a, CiTLR22b, and CiTLR19 were aligned and predicted. The results showed that all the TLRs, except TLR19 whose adaptor is TRIF,[12] exhibit the conserved proline in the BB-loop (Figure S2), implying that MyD88 may be the adaptor of CiTLR7.

Grass carp genome encodes six TLR adaptors: MyD88, TIRAP, TRIF, SARM1, BCAP, and SCIMP. SARM1 and BCAP serve as negative regulators in TLR signaling.[7] SCIMP is a cellular membrane adaptor, directly binding to the TLR4-TIR domain in response to LPS.[6] Therefore, MyD88, TRIF, and TIRAP were chosen as candidate adaptors of CiTLR7. Firstly, colocalization was performed by confocal fluorescence microscopy (CFM). The results showed that CiTLR7 colocalizes with MyD88, not TRIF and TIRAP (Figure 4B), which implies that MyD88 may be the potential adaptor of CiTLR7. Then, co-immunoprecipitation (Co-IP) assays were carried out. The results indicated that CiTLR7 interacts with MyD88, not other candidate adaptors (Figure 4C). Sequence analysis, colocalization, and Co-IP experiments demonstrated that MyD88 is the adaptor of CiTLR7.

CiTLR7 enhances IFN response via SLC15A4/TASLa/TASLb/IRF5/IRF7 complex and pro-inflammatory cytokines via AP-1 pathway after viral RNA stimulation

To further address CiTLR7 signaling pathway, we investigated the engagement signal via the SLC15A4/TASL/IRF5 complex in TLR7 signaling pathway in mammals.[18] In grass carp genome, we identified SCL15A4 and two TASL orthologs (TASLa and TASLb). Firstly, we examined the subcellular localizations of SCL15A4, TASLa, and TASLb. CFM assays showed that SCL15A4 (green), TASLa (green), and TASLb (green) were overlapped with LAMP2 (red) (Figure 5A), which indicated that SCL15A4, TASLa, and TASLb locate at lysosome. Then, we checked the interaction between TASLa/TASLb and SLC15A4. We co-transfected plasmids SLC15A4-GFP, TASLa-Myc, and TASLb-Myc into FHM cells, respectively. Co-IP assays showed that SLC15A4 interacts with TASLa and TASLb (Figure 5B). After that, we explored the interactions between IRFs and TASLa/b. IRF3 and IRF7 play important roles in antiviral immunity.[35] IRF5 can be recruited by TASL in mammals.[18] We co-transfected FHM cells with TASLa-GFP, TASLb-GFP, IRF3-Flag, IRF5-Flag, and IRF7-Flag, respectively. Co-IP assays showed that IRF3 cannot interact with both TASLa and TASLb (Figure 5C), and IRF5 and IRF7 can interact with both TASLa and TASLb (Figures 5D and 5E). The results indicated that SLC15A4/TASLa/TASLb/IRF5/IRF7 complex is an important component in CiTLR7 pathway.

Furthermore, we investigated the interaction mechanism between TASLa/b and IRF5/7. TASL contains a pLxIS motif that mediates the recruitment and activation of IRF5 in mammals.[18] Firstly, we employed and compared CiTASLa, CiTASLb, HsTASL, CiIRF3, HsIRF3, CiIRF5, HsIRF5, CiIRF7, and HsIRF7 protein sequences. Multiple sequence alignment showed that all the TASLs, HsIRF3, IRF5s, and CiIRF7 sequences contain pLxIS motif, not CiIRF3 and HsIRF7 (Figure 6A). Further, we replaced the pLxIS motif with AAAAA (Alanine) in CiTASLa and CiTASLb (Figure 6B) and performed Co-IP assays. The results indicated that the mutants abolish the interactions between TASLa/b and IRF5/7 (Figures 6C and 6D). Furthermore, we checked the IFN1 promoter activity. The results showed that the mutants of CiTASLa/b very significantly reduce the IFN1 promoter activity post-R848 stimulation in CiTLR7 pathway (Figure 6E). All the results indicated that the pLxIS motif in TASLa and TASLb plays a key role in the recruitment and activation of IRF5 and IRF7 in CiTLR7 pathway.

IFN, NF-κB, and AP-1 are key molecules involved in MAMP-triggered immune responses. To explore the roles of IFN, NF-κB, and AP-1 in ssRNA- and dsRNA-triggered CiTLR7 pathway, DLR assay was firstly performed. The promoter activities of IRF5, IRF7, IFN1, IFN3, and AP-1/JunD were significantly increased in CiTLR7 overexpression cells after R848 and poly(I:C) stimulation, not IRF3, IFN2, IFN4, NF-κB1, and NF-κB2 (Figures 1H and 7A–7I). IFN1 and IFN3 were selected to verify the results after SVCV or GCRV infection; we obtained the similar trends (Figures 7J and 7K). Then, qRT-PCR was carried out. Compared with control, CiTLR7 overexpression significantly enhances mRNA expressions of IRF5, IRF7, IFN1, IFN3, IFNγ2, AP-1/JunD, IL-1β, not IRF3, IFN2, IFN4, IFNγ1, NF-κB1, and NF-κB2 at different time points post-GCRV challenge (Figure S3). All the results indicated that CiTLR7 plays a positive role in IFN and AP-1 pathways.
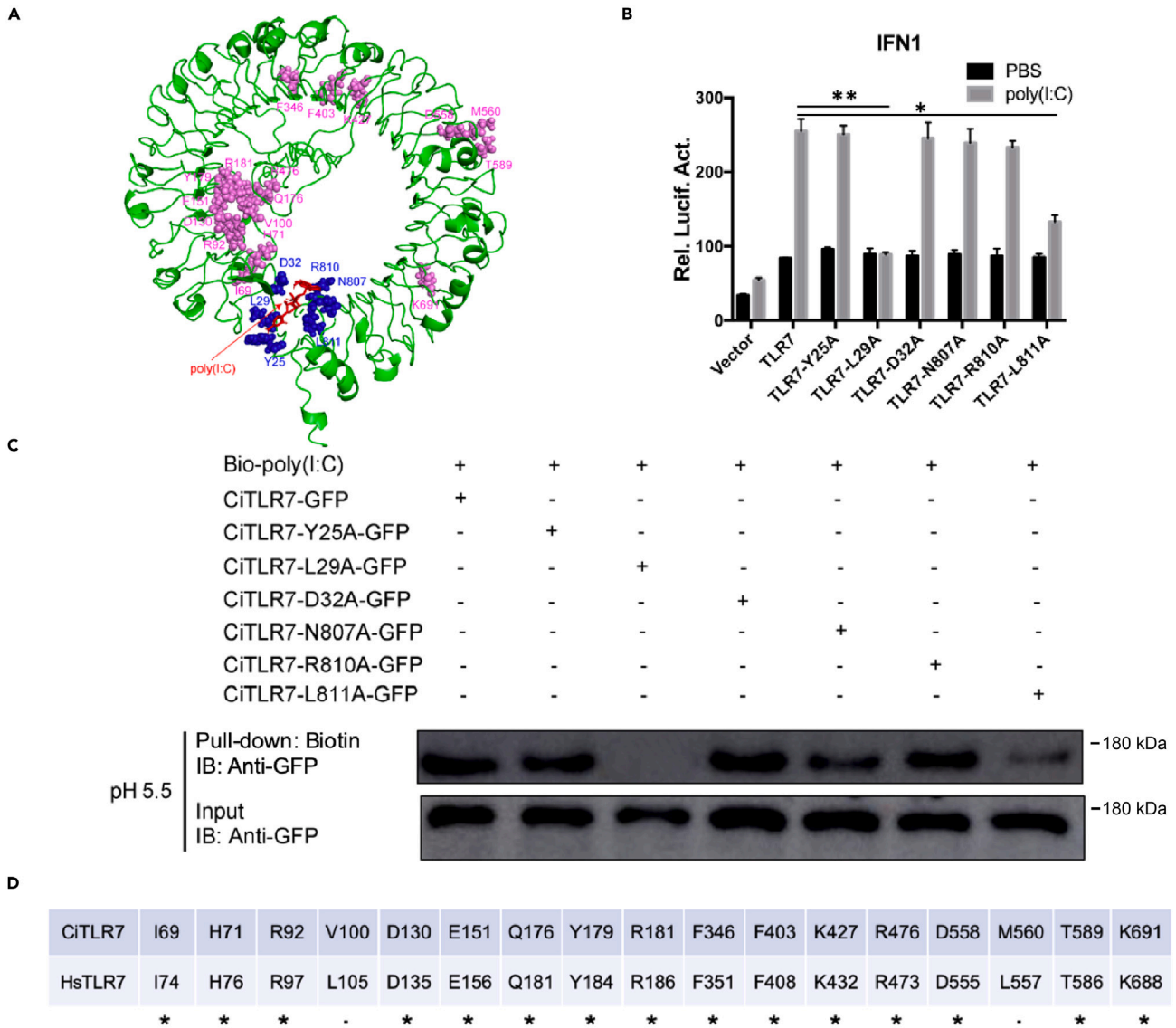
Figure 3. The binding sites of CiTLR7 with dsRNA and ssRNA

(A) Alphafold2, AutoDock Vina, and PyMOL software were employed to predict and show the binding sites of CiTLR7 with poly(I:C) as well as ssRNA. The predicted binding sites of CiTLR7 for poly(I:C) were shown in blue beads with amino acid positions. The poly(I:C) was shown in red sticks. The predicted binding sites of CiTLR7 for ssRNA were shown in pink spheres with amino acid positions.

(B) FHM cells were transfected with predicted poly(I:C) binding site mutants of CiTLR7 for 24 h and then stimulated with poly(I:C) for 24 h. Vector was used as a control. IFN1 promoter activity was examined by DLR assay (n = 3).

(C) Lysates of FHM cells overexpressing predicted poly(I:C) binding site mutants were incubated with biotin-poly(I:C) (1 μg/mL) at pH 5.5 for 1 h at 4°C; mixed with streptavidin agarose beads for 2 h at 4°C; and centrifuged, washed, denatured, and analyzed by IB with anti-GFP Ab.

(D) The predicted ssRNA-binding sites in grass carp TLR7 were aligned with the identified ssRNA-binding sites in human TLR7, which are highly conserved.

The function on binding dsRNA by TLR7 emerges in pisciformes and disappears in tetrapods

CiTLR7 senses dsRNA as mentioned earlier. We wondered how this function is in evolution. Firstly, we employed the representative vertebrate TLR7 protein sequences from northeast Chinese lamprey (LmTLR7a and LmTLR7b), zebrafish (DrTLR7), African clawed frog (XlTLR7), green anole (AcTLR7), chicken (GgTLR7), and mouse (MmTLR7) to construct the phylogenetic tree and found TLR7s cluster in consensus with taxonomic evolution (Figure 8A). Then, pull-down assays of LmTLR7a, LmTLR7b, CiTLR7, DrTLR7, XlTLR7, AcTLR7, GgTLR7, and MmTLR7 were performed using biotin-poly(I:C) as bait at pH 5.5 and pH 7.4. IBs showed that LmTLR7b, CiTLR7, and DrTLR7 interact with biotin-poly(I:C) at pH 5.5, not others (Figure 8B). However, both LmTLR7a and LmTLR7b can interact with biotin-ssRNA at pH 5.5, not pH 7.4 (Figure 8C). Correspondingly, LmTLR7b can up-regulate IFN1 and AP-1/JunD expression post-poly(I:C) stimulation (Figures 8D and 8E). Both
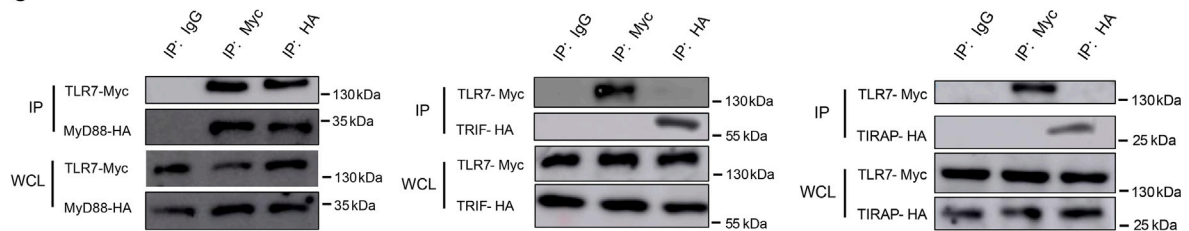
A
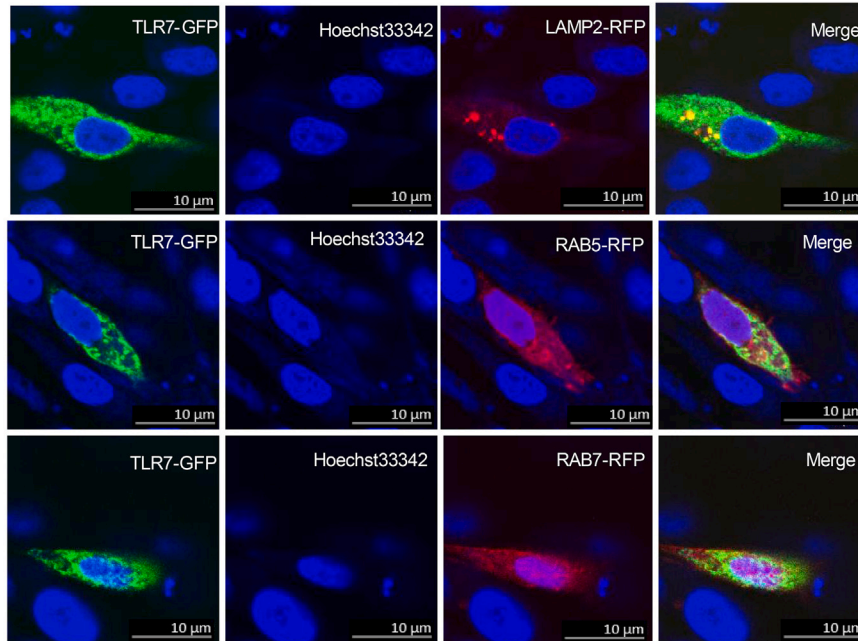
B
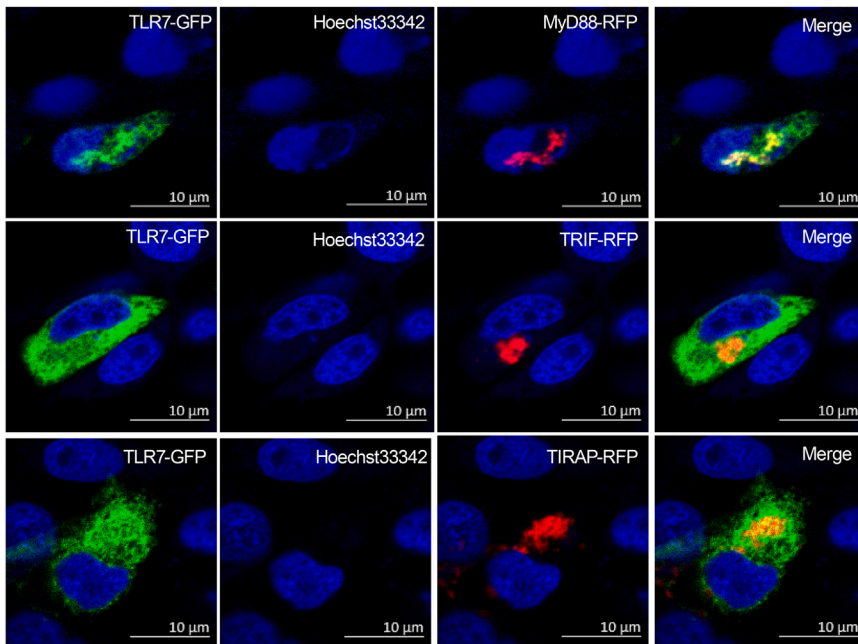
C

Figure 4. CiTLR7 locates at lysosome and recruits MyD88 as adaptor

(A) CIK cells were transfected with CiTLR7-GFP and LAMP2-RFP, a lysosome protein marker, RAB5-RFP, an early endosome protein marker, or RAB7-RFP, a late endosome protein marker, respectively, seeded on microscope cover glasses in 12-well plate for 24 h, and then stained with Hoechst33342 for 10 min and examined by CFM. Green represents CiTLR7-GFP; red stands for RAB5-RFP, RAB7-RFP, or LAMP2-RFP; and blue indicates nuclei. Yellow shows co-localization between CiTLR7 and lysosome.

(B) CIK cells were transfected with CiTLR7-GFP and MyD88-RFP, TRIF-RFP, or TIRAP-RFP, respectively, seeded on microscope cover glasses in 12-well plate for 24 h and stained with Hoechst33342 for 10 min and examined by CFM. Green represents CiTLR7-GFP; red shows MyD88-RPF, TRIF-RFP, or TIRAP-RFP; and blue indicates nuclei. Yellow stands for co-localization between CiTLR7 and MyD88.

(C) FHM cells in 10-cm^2 dishes were co-transfected with the indicated plasmids for 24 h; then IP was performed with indicated Abs. Mouse IgG was used as a control. IB was done with anti-HA and anti-Myc Abs, respectively. All the experiments were repeated at least three times.

LmTLR7a and LmTLR7b can suppress ssRNA virus proliferation (Figure 8F); just LmTLR7b inhibits dsRNA virus proliferation (Figure 8G). In addition, LmTLR7b can resist bacterial proliferation post-poly(I:C) stimulation (Figures 8H and 8I). The results demonstrated that the novel function on sensing dsRNA by TLR7 emerges in pisciformes and disappears in tetrapods in evolution.

According to our results and the literature, we proposed the schematic model to illustrate how TLR7 regulates the immune signaling pathways (Figure 9).

DISCUSSION

TLRs recognize MAMPs, subsequently trigger the innate immune signaling cascade, and activate the adaptive immunity. TLRs highly express in immune cells, such as macrophages and dendritic cells, which are professional antigen-presenting cells with the productions of inflammatory cytokines and type I IFNs. TLR7 and TLR8 recognize ssRNA. Human TLR7, TLR8, and mouse TLR7 also recognize imidazoquinoline derivatives such as R837 (imiquimod), R848, and guanine analogues, whereas mouse TLR8 does not. Mice deficient in either the TLR7 or the adaptor MyD88 demonstrate reduced responses to ssRNA virus infections.[36] In addition, TLR7 detects bacterial ssRNAs from strains such as group B *Streptococci*. However, it is not able to sense ssRNAs from other bacteria such as *Listeria monocytogenes* and group A *Streptococci*.[37] In teleost, mRNA expression of common carp (*Cyprinus carpio*) TLR7 is remarkably up-regulated post-SVCV (an ssRNA virus) infection in head kidney.[38] In our previous study, we found grass carp TLR7 locates in chromosome 9[39] and responds to poly(I:C) (a dsRNA analogue) stimulation and GCRV (a dsRNA virus) infection,[40,41] which implies that piscine TLR7 senses different ligands. In the present study, we employed CiTLR7 as a model to address the TLR7 signaling pathways and immune functions in teleost and even other species in evolution.

Firstly, we investigated the ligands and function of CiTLR7. We challenged CIK cells with different MAMPs or viruses. qRT-PCR assays showed that mRNA expressions of CiTLR7 are upregulated post-challenge with ssRNA analogue, dsRNA analogue, ssRNA virus, and dsRNA virus, not bacterial dsDNA, LPS, and PGN, which indicated CiTLR7 responds to not only ssRNA but also dsRNA. The phenomena are accordance with the previous reports on responding to ssRNA virus for common carp TLR7 and dsRNA for grass carp TLR7.[38,40] Further, we provided the direct evidence that CiTLR7 interacts with ssRNA and dsRNA in acidic condition by pull-down assays. dsRNA is associated with most viral infections, which either constitutes the viral genome (in the case of dsRNA viruses) or is generated in host cells during viral replication.[21] Furthermore, DLR assays exhibited the IFN1 response was significantly enhanced by ssRNA and dsRNA stimulations via CiTLR7 in dose-dependent and synergistic manners. Moreover, we confirmed the antiviral function against ssRNA virus (SVCV) and dsRNA virus (GCRV) by overexpression of CiTLR7, standard plaque, viral titration, and mRNA expressions of viral genes. In addition, we verified the antiviral function by knockdown of CiTLR7 and antiviral activity assays. All these experiments solidify that piscine TLR7 can directly bind not only ssRNA but also dsRNA at different patches as a dual receptor, synergistically induces IFN expression, and enhances antiviral function. In the previous study, grass carp TLR8a could facilitate GCRV proliferation,[42] which can be an antagonist against CiTLR7 in antiviral immunity. This is the first TLR member recognizing both ssRNA and dsRNA and the first report on binding dsRNA by TLR7.

Then, we clarified the key binding sites of CiTLR7 for dsRNA. Firstly, we predicted and modeled the binding sites of CiTLR7 for dsRNA and ssRNA. Then, we mutated the predicted binding sites for dsRNA one by one and checked the regulatory function of the mutants by DLR assay. The results indicated that TLR7-L29A abolishes and TLR7-L811A reduces the IFN1 promoter activity mediated by CiTLR7 post-poly(I:C) stimulation. Further, we examined binding capacity of the mutants by pull-down assay. The results showed that TLR7-L29A abrogates and TLR7-L811A weakens the binding activity with dsRNA in acidic condition. Therefore, TLR7-L29A and TLR7-L811A are key binding sites for dsRNA, which locate at the adjacent N- and C-termini of extracellular region in CiTLR7, respectively. In addition, the binding sites for ssRNA in HsTLR7 are abundant[32] and conserved in CiTLR7 by site prediction and sequence alignment. Binding ssRNA for TLR7 is not novel function, so we did not mutate and testify the predicted binding sites one by one.

Further, we examined the subcellular localization and adaptor of CiTLR7. In mammals, TLRs are synthesized in the ER and transported to their ultimate destinations in cells, which are the plasma or endosomal membranes.[1] Sequential glycosylation of TLRs occurs as these proteins proceed from the ER to the Golgi complex.[1] TLR7-9 senses nucleic acids in endo-lysosome.[18] We found that CiTLR7 co-localizes with ER (GRP78 marker) for synthesis, Golgi apparatus (GM130 marker) for glycosylation modification, and lysosome (LAMP2 marker) for binding ssRNA and dsRNA, not early endosome (RAB5 marker) and late endosome (RAB7 marker). In the previous studies, the BB-loop of the TIR domain in TLRs was shown to interact with adaptors.[34,43] All the human TLRs, except TLR3, have a proline residue in the BB-loop, thought to bind MyD88.[33] To check CiTLR7 adaptor theoretically, the amino acid sequences and crystal structures of TIR domains of CiTLR7,
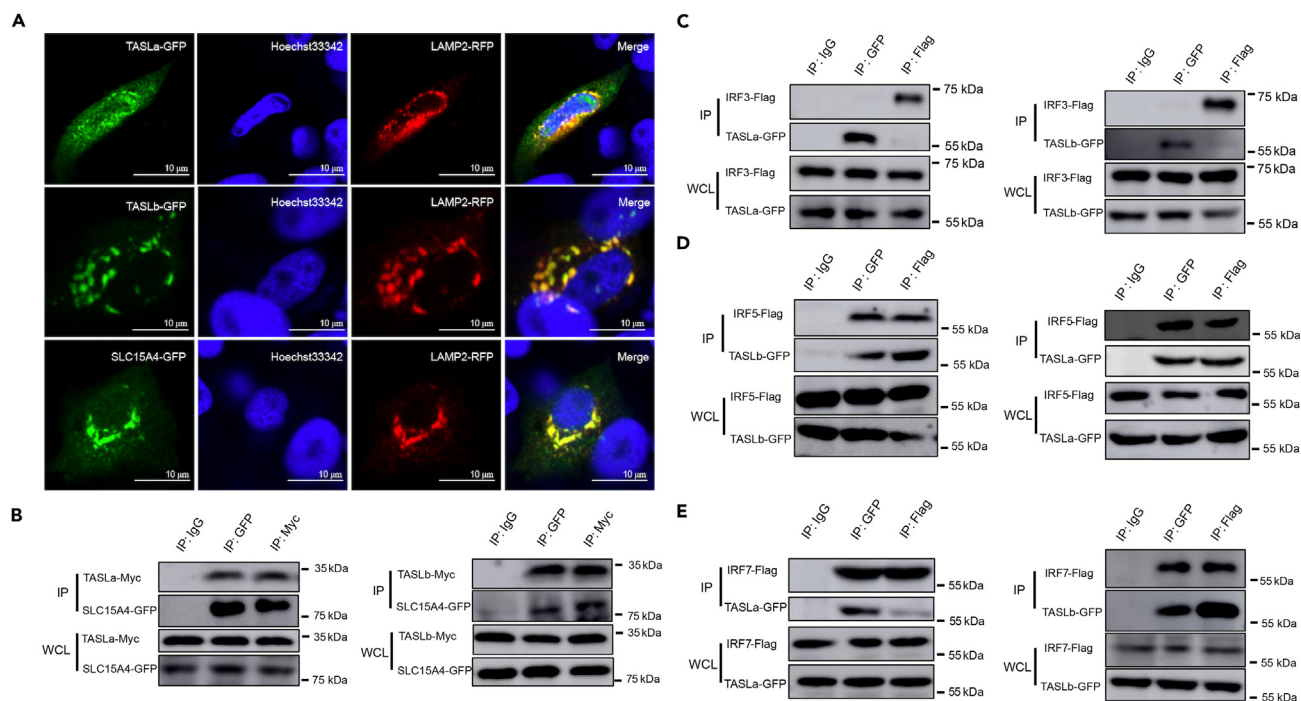
Figure 5. CiTASLa and CiTASLb recruit IRF5 and IRF7 to lysosome through SLC15A4

(A) CIK cells were co-transfected with LAMP2-RFP and CiSLC15A4, CiTASLa, or CiTASLb, respectively, seeded on microscope cover glasses in 12-well plate for 24 h, and then stained with Hoechst33342 for 10 min and examined by CFM. Green represents CiSLC15A4, CiTASLa, and CiTASLb; red stands for LAMP2-RFP; and blue indicates nuclei. Yellow shows co-localization between CiSLC15A4, CiTASLa, CiTASLb, and LAMP2.

(B) FHM cells in 10-cm^2 dishes were co-transfected with the indicated plasmids for 24 h; IP was performed with anti-GFP and anti-Myc Abs, respectively. Mouse IgG was used as a control. IB was done with anti-Myc and anti-GFP Abs, respectively.

(C–E) FHM cells in 10-cm^2 dishes were co-transfected with the indicated plasmids for 24 h; IP was performed with anti-GFP and anti-Flag Abs, respectively. Mouse IgG was used as a control. IB was done with anti-Flag and anti-GFP Abs, respectively. All the experiments were repeated at least three times.

HsTLR7, CiTLR22a, CiTLR22b, and CiTLR19 were aligned and predicted. The results showed that all the TLRs, except CiTLR19 whose adaptor is TRIF,[12] have a proline in the BB-loop, implying that MyD88 may be the adaptor of CiTLR7 in theory. Further, CFM and Co-IP assays confirmed that CiTLR7 recruits MyD88 as adaptor, not TRIF or TIRAP. In mammals, TLR7 also recruits MyD88 as adaptor.[44] These results showed that the subcellular localization and adaptor are conserved in teleosts and mammals.

Furthermore, we explored the downstream pathway molecules. TASL is an essential protein in lysosomal TLR pathway, which interacts with the lysosomal transporter SLC15A4 and contains a conserved pLxIS motif that mediates the recruitment and activation of IRF5 in mammals.[18] We identified two TASL orthologs (TASLa and TASLb) in grass carp, which co-localize with lysosome via SLC15A4; meanwhile, they interact with IRF5 and IRF7 via pLxIS motif. Noticeably, grass carp TASLa/b recruits both IRF5 and IRF7, whereas mammalian TASL just recruits IRF5, not IRF7. Further, CiTLR7 can significantly enhance the promoter activities of IRF5, IRF7, IFN1, IFN3, and AP-1/JunD, not IRF3, IFN2, IFN4, NF-κB1, or NF-κB2 after ssRNA or dsRNA stimulation, which implied that IRF5, IRF7, IFN1, IFN3, and AP-1 are in TLR7 pathways. The fact that CiTLR7 facilitates promoter activities of IFN1 and IFN3 was further testified after ssRNA and dsRNA virus infections. Furthermore, CiTLR7 can significantly boost mRNA expressions of IRF5, IRF7, IFN1, IFN3, AP-1/JunD, IFNγ2, and IL-1β, not IRF3, IFN2, IFN4, IFNγ1, NF-κB1, or NF-κB2 post-GCRV infection. Both DLR and qRT-PCR assays verified that IRF5, IRF7, IFN1, IFN3, and AP-1, not IRF3, IFN2, IFN4, or NF-κB, are in TLR7 pathways. All together, the downstream pathway molecules of CiTLR7 include SLC15A4/TASLa/TASLb/IRF5/IRF7 complex, IFN1, IFN3, and AP-1, which are different from the SLC15A4/TASL/IRF5 complex, IFNβ, AP-1, and NF-κB, in mammalian counterparts.[18,45] Actually, IFN1 possesses not only robust antiviral function but also potent antibacterial activity *in vitro* and *in vivo*.[46,47] The powerful antibacterial function of type I IFN widespreadly exists in non-mammals.[46,48] In mammals, mouse and human IFN-βs can directly kill *Staphylococcus aureus*, not *E. coli in vitro*, even only under acidic pH for human IFN-β.[49] Antibacterial immunomodulatory function is hardly detectable for mouse IFN-β *in vivo*.[47] Thus, these results indicated that both ssRNA and dsRNA trigger not only antiviral immunity but also antibacterial immunity via TLR7 in pisciformes.

Moreover, we detected the function on sensing dsRNA by TLR7 in evolution. We found that the functions of binding dsRNA and triggering downstream signaling pathway by TLR7 exist in pisciformes (Cyclostome and pisces), not tetrapods (Amphibian, reptile, aves, and mammal). Although LmTLR7a and LmTLR7b cluster together, only LmTLR7b binds dsRNA. The results indicated that TLR7 can recognize dsRNA in lower pisciformes, and the function loses in higher tetrapods.
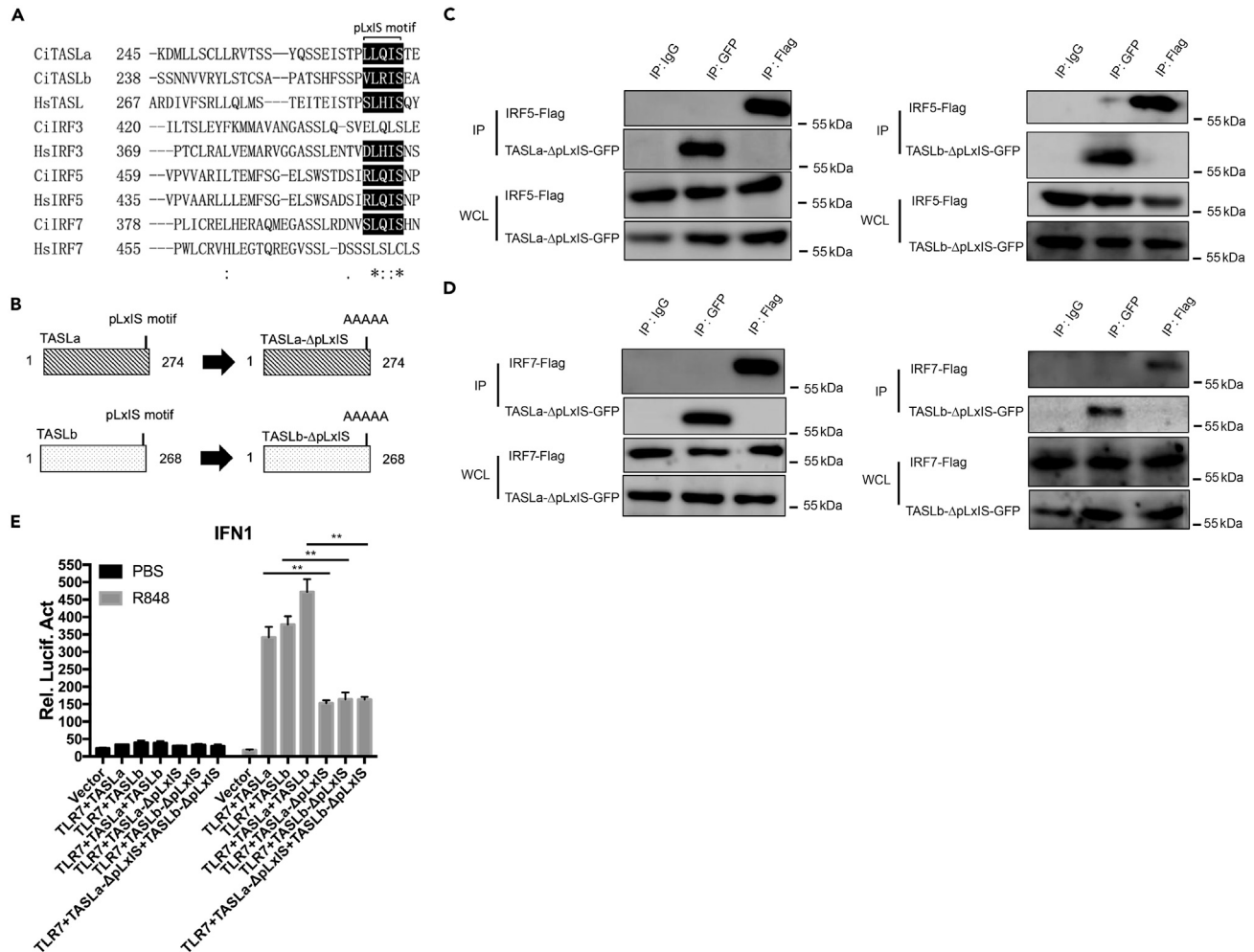
Figure 6. The pLxIS motif in TASL plays a pivotal role in recruiting IRFs and activating downstream pathway

(A) Multiple protein sequence alignment of CiTASLa, CiTASLb, HsTASL, CiIRF3, HsIRF3, CiIRF5, HsIRF5, CiIRF7, and HsIRF7 was carried out to compare the pLxIS motif regions. pLxIS motif was marked with white font and black background. Identical amino acid residues were shown by asterisks (*). High and low similarities were indicated with colons () and points (.), respectively. The protein IDs of HsTASL, HsIRF3, HsIRF5, and HsIRF7 are NP_079435, AAH71721.1, EAL24108.1, and AAI36556.1, respectively; other protein sequences are deduced from mRNA sequences in Table S1.

(B) The schematic diagram of TASLa/b mutants. The pLxIS motif was mutated into five alanines.

(C and D) FHM cells in 10-cm² dishes were co-transfected with the indicated plasmids for 24 h; IP was performed with anti-GFP and anti-Flag Abs, respectively. Mouse IgG was used as a control. IB was done with anti-Flag and anti-GFP Abs, respectively.

(E) FHM cells were transfected with the indicated plasmids for 24 h and then stimulated with R848 for 24 h. Vector was used as a control. IFN1 promoter activity was examined by DLR assay (n = 3). All the experiments were repeated at least three times. **p < 0.01.

In conclusion, TLR7 senses not only ssRNA but also dsRNA in lysosome in pisciformes and loses the function of sensing dsRNA in tetrapods. CiTLR7 shares conserved ssRNA-binding sites with HsTLR7. The key dsRNA-binding sites for CiTLR7 locate at the adjacent N-terminus (L29) and C-terminus (L811) of the ectodomain. ssRNA and dsRNA bind to CiTLR7 at different patches, thus synergistically triggering antiviral and antibacterial immunity via CiTLR7. TLR7 recruits MyD88 as adaptor in teleosts and mammals. CiTLR7 enhances IFN1 and IFN3 expression via SLC15A4/TASLa/TASLb/IRF5/IRF7 complex to activate antiviral and antibacterial immunity in teleosts, which is different from those in mammals. TLR7 boosts IFN-β expression via SLC15A4/TASL/IRF5 complex to activate antiviral immunity in mammals. TLR7 also induces pro-inflammatory cytokines via AP-1 in teleosts and AP-1 and NF-κB in mammals. The present study systematically addressed the antiviral and antibacterial functions and signaling pathways of TLR7 in teleost and found that both ssRNA and dsRNA trigger not only antiviral immunity but also antibacterial immunity via TLR7 in pisciformes. The present study provides the direct evidence that TLR7 binds ssRNA in pisciformes. This is first the evidence that TLR7 recognizes dsRNA as neofunctionalization in primitive lower pisciformes, which loses in the higher tetrapods. Also, this is the first report on sensing both ssRNA and dsRNA by a TLR member, which serves the functional evolution researches in TLRs.
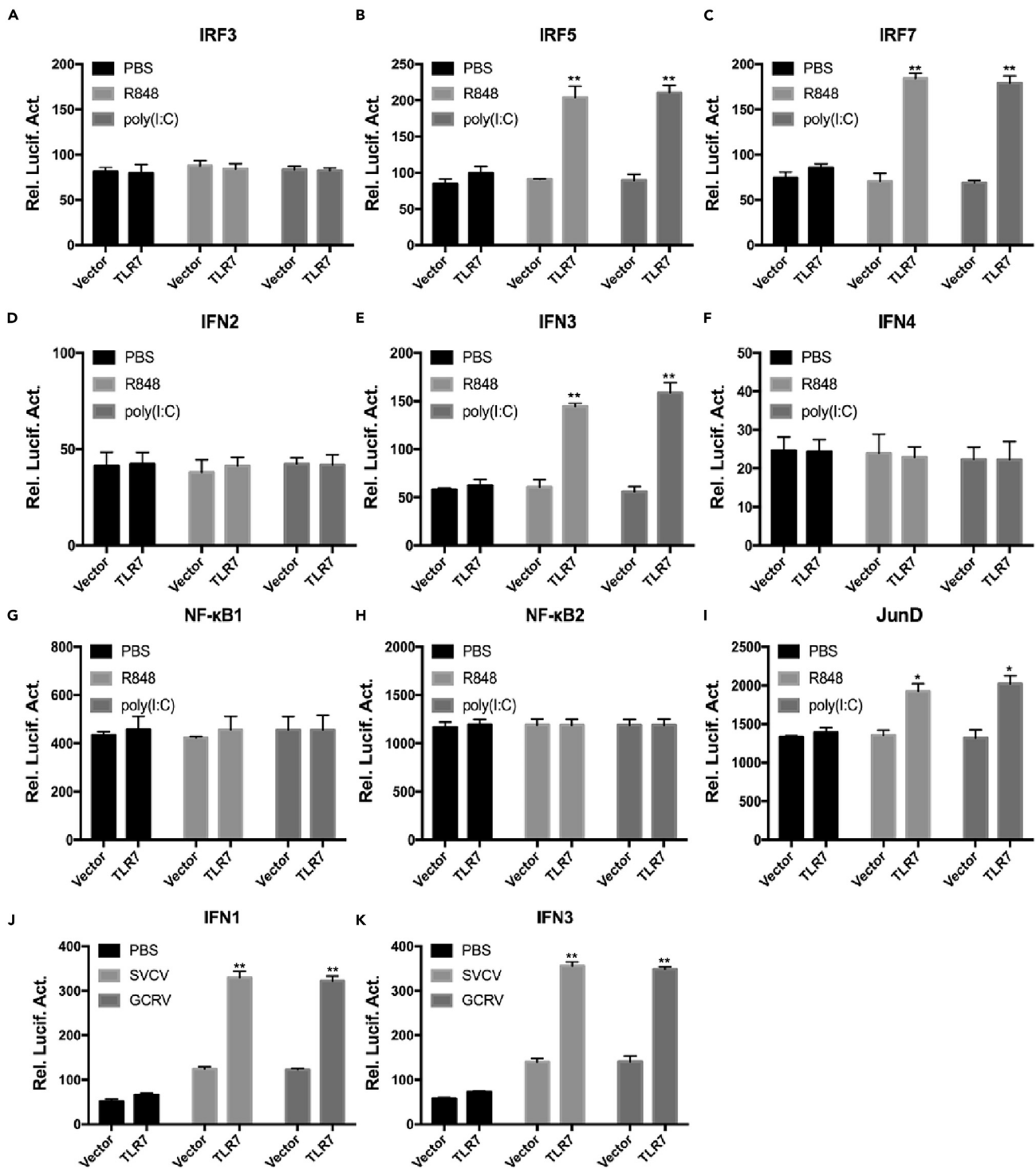
Figure 7. CiTLR7 enhances promoter activities of IRF5/7, IFN1/3, and AP-1

(A–I) FHM cells seeded in 24-well plates overnight were co-transfected with 380 ng of CiTLR7-Myc or vector, 380 ng of each target plasmid (IRF3pro-Luc, IRF5pro-Luc, IRF7pro-Luc, IFN2pro-Luc, IFN3pro-Luc, IFN4pro-Luc, NF-κB1pro-Luc, NF-κB2pro-Luc, and AP-1/JunDpro-Luc), and 38 ng pRL-TK for 24 h; the cells were stimulated with poly(I:C) or R848 for 24 h; and the luciferase activities were analyzed (n = 3).

(J and K) CIK cells were co-transfected with 380 ng of CiTLR7-Myc or vector, 380 ng of IFN1pro-Luc or IFN3pro-Luc, and 38 ng pRL-TK for 24 h and then infected with SVCV and GCRV for 24 h. IFN1 (J) and IFN3 (K) promoter activities were examined by DLR assay (n = 3). *p < 0.05, **p < 0.01.
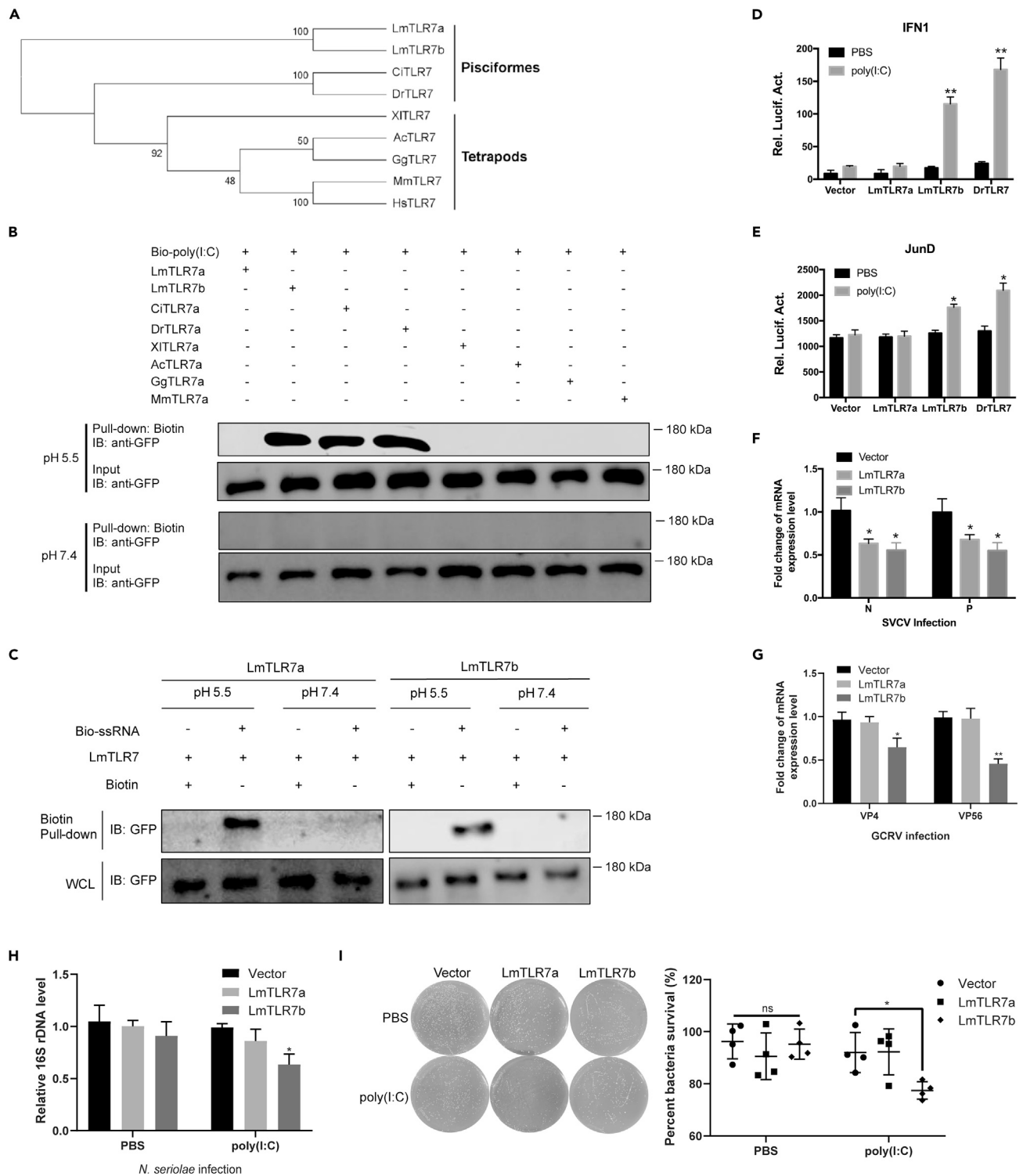
Figure 8. TLR7 binds poly(I:C) and induces antiviral and antibacterial immunities in pisciformes

(A) Representative TLR7 protein sequences were employed to construct the phylogenetic tree by neighbor-joining method within the MEGA11 program. The tree was bootstrapped 10,000 times.

(B) Lysates of FHM cells overexpressing LmTLR7a, LmTLR7b, CiTLR7, DrTLR7, XlTLR7, AcTLR7, GgTLR7, and MmTLR7 were respectively incubated with biotin-poly(I:C) (1 μg/mL) for 1 h at 4 °C at pH 5.5 and pH 7.4; mixed with streptavidin agarose beads for 2 h at 4°C; and centrifuged, washed, denatured, and analyzed by IB with anti-GFP Ab. The protein ID of HsTLR7 is AAZ99026; other protein sequences are deduced from mRNA sequences in Table S1.

Figure 8. Continued

(C) Lysates of FHM cells overexpressing LmTLR7a and LmTLR7b were respectively incubated with biotin-ssRNA (1 μg/mL) or biotin (control, 1 μg/mL) at pH 7.4 or pH 5.5 for 1 h at 4°C; mixed with streptavidin agarose beads for 2 h at 4°C; and centrifuged, washed, denatured, and analyzed by IB with anti-Myc Ab.

(D) Effects of different TLR7s on IFN1 promoter activity were measured by DLR assay in FHM cells (n = 3).

(E) Effects of different TLR7s on JunD promoter activity were measured by DLR assay in FHM cells (n = 3).

(F) FHM cells overexpressing LmTLR7a or LmTLR7b were treated with SVCV (MOI = 0.1) for 24 h, and mRNA expressions of SVCV N and P genes were measured by qRT-PCR (n = 4).

(G) FHM cells overexpressing LmTLR7a or LmTLR7b were treated with GCRV (MOI = 0.1) for 24 h, and mRNA expressions of SVCV VP4 and VP56 genes were measured by qRT-PCR (n = 4).

(H) CIK cells overexpressing constructs for 12 h and stimulated with poly(I:C) or PBS for 24 h were infected with *Nocardia seriolae* at 10^5 PFU/mL, and samples (cells and supernatants) were collected at 6 h for bacterial quantification, and 16S rDNA and EF1α were measured by qPCR (n = 4).

(I) The above samples were lysed, diluted, and plated for 7 days. The representative plates were shown (n = 4). **p < 0.01, *p < 0.05.

Limitations of the study

In the present study, we found that TLR7 senses both ssRNA and dsRNA at different regions and triggers antiviral and antibacterial immunity through SLC15A4/TASLa/TASLb/IRF5/IRF7 complex and AP-1 pathway in non-tetrapod vertebrates. The detailed protein modification regulatory mechanisms of TLR7 need to be further investigated.

STAR★METHODS

Detailed methods are provided in the online version of this paper and include the following:

- KEY RESOURCES TABLE
- RESOURCE AVAILABILITY
  - Lead contact
  - Materials availability
  - Data and code availability
- EXPERIMENTAL MODEL AND STUDY PARTICIPANT DETAILS
  - Cell lines and culture
  - Viruses and viral infections
- METHOD DETAILS
  - Protein sequence analyses and modeling
  - Plasmid constructions, RNA interference, and transfections
  - Recombinant protein expression and purification
  - Standard plaque and virus titer assays
  - Dual-luciferase reporter (DLR) and real-time quantitative RT-PCR (qRT-PCR) assays
  - Antibacterial assays
  - Pull-down, co-immunoprecipitation (Co-IP) and immunoblotting (IB)
  - Confocal fluorescence microscopy (CFM)
- QUANTIFICATION AND STATISTICAL ANALYSIS
  - Statistics

SUPPLEMENTAL INFORMATION

Supplemental information can be found online at https://doi.org/10.1016/j.isci.2023.108315.

AUTHOR CONTRIBUTIONS

Conceptualization, J.S. and R.J.; Methodology, R.J., C.Y., and Z.L.; Investigation, R.J. and W.Z.; Writing—Original Draft, J.S. and R.J.; Writing—Review & Editing, J.S.; Funding Acquisition, J.S.; Resources, Z.L. and J.S.; Supervision, J.S.

DECLARATION OF INTERESTS

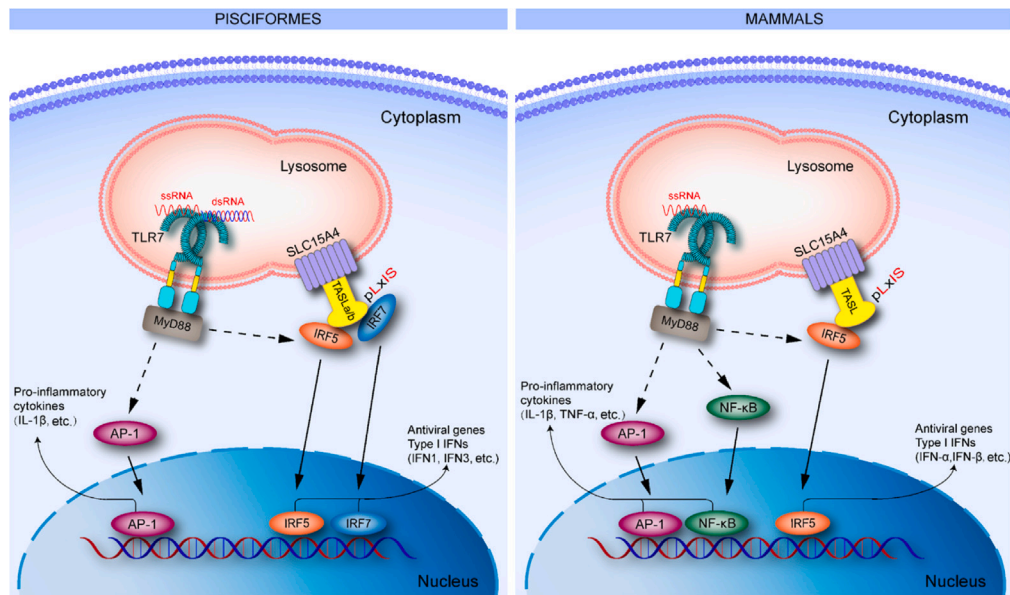The authors declare no competing interests.

Figure 9. Schematic illustrations of TLR7 signaling pathways in pisciformes and mammals

In pisciformes, TLR7 senses both ssRNA and dsRNA as a dual receptor in lysosome, recruits MyD88 as adaptor, triggers antiviral and antibacterial immunity via SLC15A4/TASLa/TASLb/IRF5/IRF7 complex, and meanwhile activates pro-inflammatory cytokines via AP-1 pathway. In contrast, mammalian TLR7 recognizes ssRNA not dsRNA in lysosome, also employs MyD88 as adaptor, induces antiviral immunity via SLC15A4/TASL/IRF5 complex, and meantime boosts pro-inflammatory cytokines via both NF-κB and AP-1 pathways.

INCLUSION AND DIVERSITY

We support inclusive, diverse, and equitable conduct of research.

REFERENCES

1. Fitzgerald, K.A., and Kagan, J.C. (2020). Toll-like receptors and the control of immunity. Cell 180, 1044–1066. https://doi.org/10.1016/j.cell.2020.02.041.

2. Akira, S., Takeda, K., and Kaisho, T. (2001). Toll-like receptors: critical proteins linking innate and acquired immunity. Nat. Immunol. 2, 675–680. https://doi.org/10.1038/90609.

3. Liao, Z., and Su, J. (2021). Progresses on three pattern recognition receptor families (TLRs, RLRs and NLRs) in teleost. Dev. Comp. Immunol. 122, 104131. https://doi.org/10.1016/j.dci.2021.104131.

4. Pasare, C., and Medzhitov, R. (2004). Toll-like receptors: linking innate and adaptive immunity. Microb. Infect. 6, 1382–1387. https://doi.org/10.1016/j.micinf.2004.08.018.

5. Liao, Z., Yang, C., Jiang, R., Zhu, W., Zhang, Y., and Su, J. (2022). Cyprinid-specific duplicated membrane TLR5 senses dsRNA as functional homodimeric receptors. EMBO Rep. 23, e54281. https://doi.org/10.15252/embr.202154281.

6. Luo, L., Bokil, N.J., Wall, A.A., Kapetanovic, R., Lansdaal, N.M., Marceline, F., Burgess, B.J., Tong, S.J., Guo, Z., Alexandrov, K., et al. (2017). SCIMP is a transmembrane non-TIR TLR adaptor that promotes proinflammatory cytokine production from macrophages. Nat. Commun. 8, 14133. https://doi.org/10.1038/ncomms14133.

7. Kanwal, Z., Wiegertjes, G.F., Veneman, W.J., Meijer, A.H., and Spaink, H.P. (2014). Comparative studies of Toll-like receptor signalling using zebrafish. Dev. Comp. Immunol. 46, 35–52. https://doi.org/10.1016/j.dci.2014.02.003.

8. Liao, Z., Wan, Q., Su, H., Wu, C., and Su, J. (2017). Pattern recognition receptors in grass carp Ctenopharyngodon idella: I. Organization and expression analysis of TLRs and RLRs. Dev. Comp. Immunol. 76, 93–104. https://doi.org/10.1016/j.dci.2017.05.019.

9. Alexopoulou, L., Holt, A.C., Medzhitov, R., and Flavell, R.A. (2001). Recognition of double-stranded RNA and activation of NF-κB by Toll-like receptor 3. Nature 413, 732–738. https://doi.org/10.1038/35099560.

10. Lee, S.M.Y., Yip, T.F., Yan, S., Jin, D.Y., Wei, H.L., Guo, R.T., and Peiris, J.S.M. (2018). Recognition of double-stranded RNA and regulation of interferon pathway by Toll-like receptor 10. Front. Immunol. 9, 516. https://doi.org/10.3389/fimmu.2018.00516.

11. Li, X.D., and Chen, Z.J. (2012). Sequence specific detection of bacterial 23S ribosomal RNA by TLR13. Elife 1, e00102. https://doi.org/10.7554/eLife.00102.

12. Ji, J., Rao, Y., Wan, Q., Liao, Z., and Su, J. (2018). Teleost-specific TLR19 localizes to endosome, recognizes dsRNA, recruits TRIF, triggers both IFN and NF-κB pathways, and protects cells from grass carp reovirus infection. J. Immunol. 200, 573–585. https://doi.org/10.4049/jimmunol.1701149.

13. Yeh, D.W., Liu, Y.L., Lo, Y.C., Yuh, C.H., Yu, G.Y., Lo, J.F., Luo, Y., Xiang, R., and Chuang, T.H. (2013). Toll-like receptor 9 and 21 have different ligand recognition profiles and cooperatively mediate activity of CpG-oligodeoxynucleotides in zebrafish. Proc. Natl. Acad. Sci. USA 110, 20711–20716. https://doi.org/10.1073/pnas.1305273110.

14. Ji, J., Liao, Z., Rao, Y., Li, W., Yang, C., Yuan, G., Feng, H., Xu, Z., Shao, J., and Su, J. (2019). Thoroughly remold the localization and signaling pathway of TLR22. Front. Immunol. 10, 3003. https://doi.org/10.3389/fimmu.2019.03003.

15. Lind, N.A., Rael, V.E., Pestal, K., Liu, B., and Barton, G.M. (2022). Regulation of the nucleic

acid-sensing Toll-like receptors. Nat. Rev. Immunol. *22*, 224–235. https://doi.org/10.1038/s41577-021-00577-0.

16. Murayama, G., Furusawa, N., Chiba, A., Yamaji, K., Tamura, N., and Miyake, S. (2017). Enhanced IFN-α production is associated with increased TLR7 retention in the lysosomes of palasmacytoid dendritic cells in systemic lupus erythematosus. Arthritis Res. Ther. *19*, 234. https://doi.org/10.1186/s13075-017-1441-7.

17. Tohme, M., Maisonneuve, L., Achour, K., Dussiot, M., Maschalidi, S., and Manoury, B. (2020). TLR7 trafficking and signaling in B cells is regulated by the MHCII-associated invariant chain. J. Cell Sci. *133*, jcs236711. https://doi.org/10.1242/jcs.236711.

18. Heinz, L.X., Lee, J., Kapoor, U., Kartnig, F., Sedlyarov, V., Papakostas, K., César-Razquin, A., Essletzbichler, P., Goldmann, U., Stefanovic, A., et al. (2020). TASL is the SLC15A4-associated adaptor for IRF5 activation by TLR7-9. Nature *581*, 316–322. https://doi.org/10.1038/s41586-020-2282-0.

19. Diebold, S.S., Kaisho, T., Hemmi, H., Akira, S., and Reis e Sousa, C. (2004). Innate antiviral responses by means of TLR7-mediated recognition of single-stranded RNA. Science *303*, 1529–1531. https://doi.org/10.1126/science.1093616.

20. Heil, F., Hemmi, H., Hochrein, H., Ampenberger, F., Kirschning, C., Akira, S., Lipford, G., Wagner, H., and Bauer, S. (2004). Species-specific recognition of single-stranded RNA via toll-like receptor 7 and 8. Science *303*, 1526–1529. https://doi.org/10.1126/science.1093620.

21. Chen, Y.G., and Hur, S. (2022). Cellular origins of dsRNA, their recognition and consequences. Nat. Rev. Mol. Cell Biol. *23*, 286–301. https://doi.org/10.1038/s41580-021-00430-1.

22. Weber, F., Wagner, V., Rasmussen, S.B., Hartmann, R., and Paludan, S.R. (2006). Double-stranded RNA is produced by positive-strand RNA viruses and DNA viruses but not in detectable amounts by negative-strand RNA viruses. J. Virol. *80*, 5059–5064. https://doi.org/10.1128/jvi.80.10.5059-5064.2006.

23. Yamamoto, M., Sato, S., Hemmi, H., Hoshino, K., Kaisho, T., Sanjo, H., Takeuchi, O., Sugiyama, M., Okabe, M., Takeda, K., and Akira, S. (2003). Role of adaptor TRIF in the MyD88-independent Toll-like receptor signaling pathway. Science *301*, 640–643. https://doi.org/10.1126/science.1087262.

24. Oshiumi, H., Matsumoto, M., Funami, K., Akazawa, T., and Seya, T. (2003). TICAM-1, an adaptor molecule that participates in Toll-like receptor 3-mediated interferon-β induction. Nat. Immunol. *4*, 161–167. https://doi.org/10.1038/ni886.

25. Oganesyan, G., Saha, S.K., Guo, B., He, J.Q., Shahangian, A., Zarnegar, B., Perry, A., and Cheng, G. (2006). Critical role of TRAF3 in the Toll-like receptor-dependent and -independent antiviral response. Nature *439*, 208–211. https://doi.org/10.1038/nature04374.

26. Schröder, M., Baran, M., and Bowie, A.G. (2008). Viral targeting of DEAD box protein 3 reveals its role in TBK1/IKKε-mediated IRF activation. EMBO J. *27*, 2147–2157. https://doi.org/10.1038/emboj.2008.143.

27. Liao, Z., Wan, Q., and Su, J. (2016). Bioinformatics analysis of organizational and expressional characterizations of the IFNs, IRFs and CRFBs in grass carp

Ctenopharyngodon idella. Dev. Comp. Immunol. *61*, 97–106. https://doi.org/10.1016/j.dci.2016.03.020.

28. Yanai, H., Chen, H.-m., Inuzuka, T., Kondo, S., Mak, T.W., Takaoka, A., Honda, K., and Taniguchi, T. (2007). Role of IFN regulatory factor 5 transcription factor in antiviral immunity and tumor suppression. Proc. Natl. Acad. Sci. USA *104*, 3402–3407. https://doi.org/10.1073/pnas.0611559104.

29. Jiang, Z., Mak, T.W., Sen, G., and Li, X. (2004). Toll-like receptor 3-mediated activation of NF-κB and IRF3 diverges at Toll-IL-1 receptor domain-containing adapter inducing INF-β. Proc. Natl. Acad. Sci. USA *101*, 3533–3538. https://doi.org/10.1073/pnas.0308496101.

30. Bonizzi, G., and Karin, M. (2004). The two NF-κB activation pathways and their role in innate and adaptive immunity. Trends Immunol. *25*, 280–288. https://doi.org/10.1016/j.it.2004.03.008.

31. Rimann, I., Gonzalez-Quintial, R., Baccala, R., Kiosses, W.B., Teijaro, J.R., Parker, C.G., Li, X., Beutler, B., Kono, D.H., and Theofilopoulos, A.N. (2022). The solute carrier SLC15A4 is required for optimal trafficking of nucleic acid-sensing TLRs and ligands to endolysosomes. Proc. Natl. Acad. Sci. USA *119*, e2200544119. https://doi.org/10.1073/pnas.2200544119.

32. Zhang, Z., Ohto, U., Shibata, T., Krayukhina, E., Taoka, M., Yamauchi, Y., Tanji, H., Isobe, T., Uchiyama, S., Miyake, K., and Shimizu, T. (2016). Structural analysis reveals that Toll-like receptor 7 is a dual receptor for guanosine and single-stranded RNA. Immunity *45*, 737–748. https://doi.org/10.1016/j.immuni.2016.09.011.

33. Verstak, B., Arnot, C.J., and Gay, N.J. (2013). An alanine-to-proline mutation in the BB-loop of TLR3 Toll/IL-1R domain switches signalling adaptor specificity from TRIF to MyD88. J. Immunol. *191*, 6101–6109. https://doi.org/10.4049/jimmunol.1300849.

34. Enokizono, Y., Kumeta, H., Funami, K., Horiuchi, M., Sarmiento, J., Yamashita, K., Standley, D.M., Matsumoto, M., Seya, T., and Inagaki, F. (2013). Structures and interface mapping of the TIR domain-containing adaptor molecules involved in interferon signaling. Proc. Natl. Acad. Sci. USA *110*, 19908–19913. https://doi.org/10.1073/pnas.1222811110.

35. Sato, M., Suemori, H., Hata, N., Asagiri, M., Ogasawara, K., Nakao, K., Nakaya, T., Katsuki, M., Noguchi, S., Tanaka, N., and Taniguchi, T. (2000). Distinct and essential roles of transcription factors IRF-3 and IRF-7 in response to viruses for IFN-α/β gene induction. Immunity *13*, 539–548. https://doi.org/10.1016/s1074-7613(00)00053-4.

36. Lund, J.M., Alexopoulou, L., Sato, A., Karow, M., Adams, N.C., Gale, N.W., Iwasaki, A., and Flavell, R.A. (2004). Recognition of single-stranded RNA viruses by Toll-like receptor 7. Proc. Natl. Acad. Sci. USA *101*, 5598–5603. https://doi.org/10.1073/pnas.0400937101.

37. Mancuso, G., Gambuzza, M., Midiri, A., Biondo, C., Papasergi, S., Akira, S., Teti, G., and Beninati, C. (2009). Bacterial recognition by TLR7 in the lysosomes of conventional dendritic cells. Nat. Immunol. *10*, 587–594. https://doi.org/10.1038/ni.1733.

38. Wei, X., Li, X.Z., Zheng, X., Jia, P., Wang, J., Yang, X., Yu, L., Shi, X., Tong, G., and Liu, H. (2016). Toll-like receptors and interferon associated immune factors responses to spring viraemia of carp virus infection in common carp (*Cyprinus carpio*). Fish Shellfish

Immunol. *55*, 568–576. https://doi.org/10.1016/j.fsi.2016.05.043.

39. Wu, C.S., Ma, Z.Y., Zheng, G.D., Zou, S.M., Zhang, X.J., and Zhang, Y.A. (2022). Chromosome-level genome assembly of grass carp (*Ctenopharyngodon idella*) provides insights into its genome evolution. BMC Genom. *23*, 271. https://doi.org/10.1186/s12864-022-08503-x.

40. Yang, C., Su, J., Zhang, R., Peng, L., and Li, Q. (2012). Identification and expression profiles of grass carp *Ctenopharyngodon idella* TLR7 in responses to double-stranded RNA and virus infection. J. Fish. Biol. *80*, 2605–2622. https://doi.org/10.1111/j.1095-8649.2012.03316.x.

41. Su, J.J., Shang, X.Y., Wan, Q.Y., and Su, J.G. (2018). SNP-based susceptibility-resistance association and mRNA expression regulation analyses of TLR7 to grass carp *Ctenopharyngodon idella* reovirus. J. Fish. Biol. *92*, 1505–1525. https://doi.org/10.1111/jfb.13607.

42. Chen, X., Wang, Q., Yang, C., Rao, Y., Li, Q., Wan, Q., Peng, L., Wu, S., and Su, J. (2013). Identification, expression profiling of a grass carp TLR8 and its inhibition leading to the resistance to reovirus in CIK cells. Dev. Comp. Immunol. *41*, 82–93. https://doi.org/10.1016/j.dci.2013.04.015.

43. Vyncke, L., Bovijn, C., Pauwels, E., Van Acker, T., Ruyssinck, E., Burg, E., Tavernier, J., and Peelman, F. (2016). Reconstructing the TIR side of the myddosome: a paradigm for TIR-TIR interactions. Structure *24*, 437–447. https://doi.org/10.1016/j.str.2015.12.018.

44. O'Neill, L.A.J., Golenbock, D., and Bowie, A.G. (2013). The history of Toll-like receptors - redefining innate immunity. Nat. Rev. Immunol. *13*, 453–460. https://doi.org/10.1038/nri3446.

45. Wan, Q., Wang, H., Han, X., Lin, Y., Yang, Y., Gu, L., Zhao, J., Wang, L., Huang, L., Li, Y., and Yang, Y. (2014). Baicalin inhibits TLR7/MyD88 signaling pathway activation to suppress lung inflammation in mice infected with influenza A virus. Biomed. Rep. *2*, 437–441. https://doi.org/10.3892/br.2014.253.

46. Xiao, X., Zhu, W., Zhang, Y., Liao, Z., Wu, C., Yang, C., Zhang, Y., Xiao, S., and Su, J. (2021). Broad-spectrum robust direct bactericidal activity of fish IFNφ1 reveals an antimicrobial peptide-like function for type I IFNs in vertebrates. J. Immunol. *206*, 1337–1347. https://doi.org/10.4049/jimmunol.2000680.

47. Zhu, W., Zhang, Y., Liao, Z., Huo, X., Yang, C., Zhang, Y., and Su, J. (2023). IFN1 enhances thrombocyte phagocytosis through IFN receptor complex-JAK/STAT-complement C3.3-CR1 pathway and facilitates antibacterial immune regulation in teleost. J. Immunol. *210*, 1043–1058. https://doi.org/10.4049/jimmunol.2200787.

48. Su, J. (2022). The discovery of type IV interferon system revolutionizes interferon family and opens up a new frontier in jawed vertebrate immune defense. Sci. China Life Sci. *65*, 2335–2337. https://doi.org/10.1007/s11427-022-2112-0.

49. Kaplan, A., Lee, M.W., Wolf, A.J., Limon, J.J., Becker, C.A., Ding, M., Murali, R., Lee, E.Y., Liu, G.Y., Wong, G.C.L., and Underhill, D.M. (2017). Direct antimicrobial activity of IFN-β. J. Immunol. *198*, 4036–4045. https://doi.org/10.4049/jimmunol.1601226.

50. Fan, C., Su, H., Liao, Z., Su, J., Yang, C., Zhang, Y., and Su, J. (2021). Teleost-specific MxG, a traitor in the Mx family, negatively

regulates antiviral responses by targeting IPS-1 for proteasomal degradation and STING for lysosomal degradation. J. Immunol. *207*, 281–295. https://doi.org/10.4049/jimmunol.2000555.

51. Morris, G.M., Huey, R., Lindstrom, W., Sanner, M.F., Belew, R.K., Goodsell, D.S., and Olson, A.J. (2009). AutoDock4 and AutoDockTools4: automated docking with selective receptor flexibility. J. Comput. Chem. *30*, 2785–2791. https://doi.org/10.1002/jcc.21256.

52. Trott, O., and Olson, A.J. (2010). Software news and update AutoDock Vina: improving the speed and accuracy of docking with a new scoring function, efficient optimization, and multithreading. J. Comput. Chem. *31*, 455–461. https://doi.org/10.1002/jcc.21334.

53. Rao, Y., Wan, Q., Yang, C., and Su, J. (2017). Grass carp laboratory of genetics and physiology 2 serves as a negative regulator in retinoic acid-inducible gene I- and melanoma differentiation-associated gene 5-mediated antiviral signaling in resting state and early stage of grass carp reovirus infection. Front. Immunol. *8*, 352. https://doi.org/10.3389/fimmu.2017.00352.

54. Su, J., Zhang, R., Dong, J., and Yang, C. (2011). Evaluation of internal control genes for qRT-PCR normalization in tissues and cell culture for antiviral studies of grass carp (*Ctenopharyngodon idella*). Fish Shellfish Immunol. *30*, 830–835. https://doi.org/10.1016/j.fsi.2011.01.006.

STAR★METHODS

KEY RESOURCES TABLE

REAGENT or RESOURCE	SOURCE	IDENTIFIER
Antibodies		
Mouse anti-GFP monoclonal Ab	Abcam	Cat# ab291; RRID: AB_449092
Mouse anti-HA monoclonal Ab	Abcam	Cat# ab18181; RRID: AB_444303
Mouse anti-Flag monoclonal Ab	Creative Biomart	Cat# CAB551; RRID: AB_10805068
Mouse anti-Myc monoclonal Ab	Abcam	Cat# ab18185; RRID: AB_444307
Rabbit anti-β-tubulin polyclonal Ab	Bioss	Cat# bs-0210R; RRID: AB_10855547
Mouse anti-GST monoclonal Ab	Biosensis	Cat# M-1306-100; RRID: AB_2492469
Goat anti-mouse Ig-HRP conjugate secondary Ab	GenWay Biotech Inc	Cat# GWB-8D59FF; RRID: AB_10274766
Goat anti-rabbit Ig-HRP conjugate secondary Ab	ECM Biosciences	Cat# RS3201; RRID: AB_715256
Bacterial and virus strains		
Aeromonas hydrophila	ATCC	7966
Nocardia seriolae	Isolation and identification by our lab	N/A
GCRV-GZ1208	Liao et al.[5]	N/A
SVCV	Fan et al.[50]	N/A
Chemicals and recombinant proteins		
LPS from *E.coli* 0111:B4	Sigma-Aldrich	L4391
PGN form *Micrococcus luteus*	Sigma-Aldrich	53243
poly(I:C)	Sigma-Aldrich	P9582
Biotin-poly(I:C) (HMW)	InvivoGen	tlrl-picb
Biotin-ssRNA	GenePharma	N/A
R848 (Resiquimod)	InvivoGen	tlrl-r848
Isopropyl β-D-1-thiogalactopyranoside (IPTG)	Sigma-Aldrich	I6758
Hoechst 33342	AAT Bioquest	17530
FuGENE 6	Promega	E2691
Restriction enzymes	Thermo Fisher Scientifc	N/A
TLR7-LRR-GST	This paper	N/A
Deposited data		
C. idella TASLa	This paper	OQ709886
C. idella TASLb	This paper	OQ709887
C. idella IRF5 promoter	This paper	OQ709888
C. idella JunD promoter	This paper	OQ726124
Experimental models: Cell lines		
CIK	CCTCC	GDC0086
FHM	ATCC	CCL-42
Oligonucleotides		
Primers for vector constructions and qRT-PCR assays, See Table S1	Tsingke Biotechnology Co., Ltd	N/A
Software and algorithms		
GraphPad Prism v8.0	GraphPad	https://www.graphpad.com
Clustal Omega	EMBL-EBI	https://www.ebi.ac.uk/Tools/msa/clustalo/

(Continued on next page)

Continued		
REAGENT or RESOURCE	SOURCE	IDENTIFIER
MEGA11	MEGA	https://www.megasoftware.net/
SWISS-MODEL	Expasy	https://swissmodel.expasy.org/
PyMOL	Schrödinger	http://www.pymol.org

RESOURCE AVAILABILITY

Lead contact

Further information and requests for resources and reagents should be directed to and will be fulfilled by the Lead Contact, Jianguo Su (sujianguo@mail.hzau.edu.cn).

Materials availability

The materials underlying this article will be shared upon request to the lead contact.

Data and code availability

- New nucleotide sequences presented in this article have been deposited in GenBank under Accession numbers: OQ709886 for *C. idella* TASLa; OQ709887 for *C. idella* TASLb; OQ709888 for *C. idella* IRF5 promoter; OQ726124 for *C. idella* JunD promoter.
- The dataset is publicly available as of the date of publication.
- This study does not report original code.
- All data reported in this study and any additional information required to reanalyze the data is available from the lead contact upon request.

EXPERIMENTAL MODEL AND STUDY PARTICIPANT DETAILS

Cell lines and culture

CIK and FHM cells were obtained from China Center for Type Culture Collection (CCTCC GDC0086) and American Type Culture Collection (ATCC CCL-42), and respectively cultured in DMEM (Gibco, USA) and M199 (Gibco) mediums supplemented with 10% fetal bovine serum (Gibco), 100 U/ml penicillin (Sigma, USA), and 100 μg/ml streptomycin (Sigma) at 28°C with a 5% CO_2 incubator.

Viruses and viral infections

GCRV-GZ1208, a type I GCRV strain, and SVCV, are common aquatic animal viruses, preserved in our lab and used for infection experiments at a multiplicity of infection (MOI) of 0.1.

METHOD DETAILS

Protein sequence analyses and modeling

Multiple protein sequence alignments were performed using Clustal Omega (https://www.ebi.ac.uk/Tools/msa/clustalo/) with default settings. Phylogenetic tree was constructed using MEGA11 (https://www.megasoftware.net/). Signal peptide was predicted using Signal-3L 3.0 (http://www.csbio.sjtu.edu.cn/bioinf/Signal-3L/) with default settings. LRR was identified using the Leucine-Rich Repeat Finder (www.lrrfinder.com/lrrfinder.php). Transmembrane region was predicted with TMHMM Server version 2.0 (www.cbs.dtu.dk/services/TMHMM/). TIR domain was predicted using the Proteus Protein Structure Prediction Server (www.proteus2.ca/proteus2/).

Structural model of CiTLR7 ectodomain was predicted by AlphaFold2 and visualized by Chimera (Version 1.15). The 2D structure of poly(I:C) dimer (CID: 136374402) was obtained from the NCBI PubChem database (http://pubchem.ncbi.nlm.nih.gov/), and the 3D structure was generated using the PRODRG2 server (http://davapc1.bioch.dundee.ac.uk/cgi-bin/prodrg/). To calculate the binding energy, polar hydrogens were added to the CiTLR7-ectodomain using AutoDockTools 1.5.6.[51] AutoDock Vina was used for docking the potential interactions of amino acids. The 3D affinity grid field was created using the auxiliary program Auto-Grid. A grid system of (x, y, z) = (100-point, 100-point, 100-point) and grid spacing of 0.575 Å were considered for docking calculations.[52] The 3D model of the CiTLR7-ectodomain, along with the docking results, were graphically presented using PyMOL (http://www.pymol.org).

Plasmid constructions, RNA interference, and transfections

pCMV-eGFP, pCMV-RFP, pcDNA4.0 and pCMV-eGFP-CMV-SV40 plasmids were employed for the constructions of expression vectors. For subcellular localization experiments, the full-length open reading frames of CiTLR7, CiSLC15A4, CiTASLa, CiTASLb, GRP78, GM130 were amplified with corresponding primers (Table S1), digested with restriction enzymes, and ligated into pCMV-eGFP and pCMV-RFP digested by the corresponding enzymes for constructing pCiTLR7-GFP, pCiSLC15A4-GFP, pCiTASLa-GFP, pCiTASLb-GFP, pCiGRP78-RFP, pCiGM130-RFP fusion vectors, respectively. CiTLR7-Myc, CiTASLa-Myc and CiTASLb-Myc were ligated into pcDNA4.0 to construct small

tag fusion vectors. CiIRF5-Flag was ligated into pCMV-eGFP-CMV-SV40 to construct small tag fusion vector. CiTLR7, CiTASLa and CiTASLb mutants were generated using PCR-based, site-directed mutagenesis and overlap PCR. TLR7 members from northeast Chinese lamprey (*Lethenteron morii*), zebrafish (*D. rerio*), African clawed frog (*Xenopus laevis*), green anole (*Anolis carolinensis*), chicken (*Gallus gallus*) and mouse (*M. musculus*) were also ligated into pCMV-eGFP to construct fusion vectors. For DLR assays, the valid promoters AP-1/JunD and IRF5 were ligated into pGL3-basci luciferase reporter vector. All the constructs were confirmed by sequencing. Other plasmids used in the present study, RAB5-RFP, RAB7-RFP, LAMP2-RFP, MyD88-RFP, TRIF-RFP, TIRAP-RFP, MyD88-HA, TRIF-HA, TIRAP-HA, CiIRF3-Flag, CiIRF7-Flag, IRF3 promoter-Luc, IRF7 promoter-Luc, IFN1 promoter-Luc, IFN2 promoter-Luc, IFN3 promoter-Luc, IFN4 promoter-Luc, NF-κB1 promoter-Luc, NF-κB2 promoter-Luc, were previously constructed in our laboratory.[14,53]

To knock down mRNA expression of CiTLR7, 3 siRNA sequences (S1: 5′-GCAACAAGUCAUACUACAUUTT-3′; S2: 5′-GCUUGAUCAUUCUG GAUAUUTT-3′; S3: 5′-AGUUAAUCAUGAACGACAAUTT-3′) were designed and synthesized by Genepharma (China). Interfering efficiency of the 3 candidate siRNAs were evaluated by qRT-PCR at 12 h post transfection, and negative control siRNA (Control: 5′-GAGAUGUCUAUGAA CAACATT-3′) was provided by GenePharma.

Plasmids or siRNAs were transfected into CIK or FHM cells using FuGENE 6 Transfection Reagent (Promega) according to manufacturer instructions. Function investigations were performed at 24 h post transfecting overexpression plasmids, or at 12 h post transfecting siRNAs.

Recombinant protein expression and purification

The fragment encoding the ectodomain of CiTLR7 was obtained by PCR amplification with primers listed in Table S1. Afterward, purified PCR product was digested with restriction enzymes *Hin*D III and *Bam*H I and then ligated into the pGEX-4T-1 expression vector. Recombinant protein was expressed in *E. coli* BL21 (DE3) cells and purified using glutathione S-transferase-nitrilotriacetic acid (GST-NTA) beads.

Standard plaque and virus titer assays

For standard plaque assays, cells overexpressed CiTLR7, interfering CiTLR7, or blank vector were severally seeded in 24-well plate (5 × 10^5 cells/well) overnight, infected with serial-diluted GCRV or SVCV at indicated dilution for 48 h, fixed with 10% paraformaldehyde for 10min at room temperature and stained with 0.05% (wt/vol) crystal violet (Sigma) for 30min, then washed with water and drained. Subsequently, the plate was photographed under a light box (Bio-Rad).

For viral titer assays, samples (1 × 10^6 cells per well) were infected with virus (MOI = 0.1) for 24 h, supernatants were serially diluted by 10-fold (10^{-1}-10^{-8}) and incubated with CIK cells in a flat 96-well plate to determine the 50% tissue culture infective dose ($TCID_{50}$). Cells were incubated at 28°C for 7 days. On day 7, the plate was examined for the presence of viral cytopathic effect (CPE) under the microscope.

Dual-luciferase reporter (DLR) and real-time quantitative RT-PCR (qRT-PCR) assays

FHM or CIK cells were seeded in 24-well plate at density of 5 × 10^5 cells/ml for 24 h. The co-transfection was performed with 380 ng expression plasmid, 380 ng target promoter-luciferase plasmid, and 38 ng pRL-TK for 24 h, stimulated with MAMPs (1 μg/ml), GCRV (MOI = 0.1), SVCV (MOI = 0.1) or PBS for 24 h. The cells were washed with PBS, lysed with Passive Lysis Buffer (Promega), and assayed for luciferase activity in luminometer (Promega). The luciferase reading of each sample was first normalized against the pRL-TK level, and the relative light unit intensity was presented as the ratio of firefly luciferase to renilla luciferase. All experiments were performed in three times.

For qRT-PCR assay, the samples were homogenized in TRIZOL LS reagent (Invitrogen). Total RNA was isolated according to the manufacturer's instruction and incubated with RNase-free DNase I (Roche) to remove contaminated genomic DNA. qRT-PCR was established in the Toche LightCycler 480II system, and EF1α was employed as an internal control gene for cDNA normalization. qRT-PCR amplification was carried out in a total volume of 15 μl, containing 7.5 μl of BioEasy Master Mix (SYBR Green) (Hangzhou Bioer Technology Co., Ltd. China), 3.1 μl of nuclease-free water, 4 μl of diluted cDNA (200 ng), and 0.2 μl of each gene specific primers (10 μM) (Table S1). The dates were analyzed using the $2^{-\Delta\Delta CT}$ method as described previously.[54]

Antibacterial assays

CiTLR7, LmTLR7a, LmTLR7b and vector were transfected into CIK cells for 12 h, then stimulated with poly(I:C) (1 μg/ml) or PBS for 24 h. Subsequently, 1 × 10^5 CFU *N. seriolae* (which grow slowly and do not increase significantly in number within 24 h) were added to the cell culture pore plate for 6 h. 50 μL supernatant was applied to the BHI (brain heart infusion, selective medium for *N. seriolae*) culture plate. The number of bacterial colonies on the plate were counted after seven days of bacterial growth (n = 4). In addition, all the samples (cells and supernatants) were collected at 6 h for bacterial quantification by qPCR. The relative expression level of 16S rDNA of *N. seriolae* was measured. EF-1α was used as the internal control gene (n = 4).

Pull-down, co-immunoprecipitation (Co-IP) and immunoblotting (IB)

For pull-down assay, FHM cells overexpressing the indicated gene were lysed in buffer (50 mM Tris-HCl, 150 mM NaCl, 5 mM EDTA, 1% IGEPAL CA-630 (pH 5.5), and Roche complete protease inhibitor cocktail) or buffer (50 mM Tris-HCl, 150 mM NaCl, 5 mM EDTA, 1% IGEPAL CA-630 (pH 7.4), and Roche complete protease inhibitor cocktail) for 30 min at 4°C with gentle rotation. Cellular debris was removed by centrifugation at 12,000 g for 30 min at 4°C. The supernatant was transferred to a fresh tube, incubated with biotin-ssRNA (5′-Biotin-GsCsCsCsGsUsCsUsGsUsUsGsUsGsUsGsAsCsUsC-3′ ("s" depicts a phosphothioate linkage))[20] or biotin-poly(I:C) (1μg/ml) for 1 h at 4°C,

and then mixed with streptavidin agarose beads for 2 h at 4°C. The beads were collected by centrifugation at 3,000 g for 5 min and washed three times with lysis buffer. Subsequently, the beads were suspended in 20 μl 2 × SDS loading buffer, denatured at 95°C for 10 min, and then analyzed by IB.

For Co-IP assay, FHM cells cultured in 10-cm^2 dishes were co-transfected with the indicated plasmids for 24 h. The cells were lysed in IP lysis buffer (20 mM Tris (pH 7.4), 150 mM NaCl, 1% Triton X-100, 1 mM EDTA, 1-mM Na$_3$VO$_4$, 0.5 μg/ml leupeptin, and 2.5 mM sodium pyrophosphate) (Beyotime) adding 1 mM phenylmethylsulfonyl fluoride (Beyotime) for 30 min at 4°C with gentle rotation, and the cellular debris was removed by centrifugation at 12,000 g for 30 min at 4°C. The supernatant was transferred to a fresh tube and incubated with 1 μg Ab with gentle shaking for 6 h at 4°C. Protein A + G sepharose beads (30 μl) (Beyotime) were added to the mixture and incubated for 2 h at 4°C. After centrifugation at 3,000 g for 5 min, the beads were then collected, washed three times with lysis buffer, suspended in 20 μl 2 × SDS loading buffer, and denatured at 95°C for 10 min, followed by IB.

For IB analysis, protein extracts were separated by 4-12% SDS-PAGE gels and transferred onto nitrocellulose membranes (Millipore, USA). The membranes were blocked in fresh 5% nonfat dry milk (dissolved in TBST buffer) overnight at 4°C and then incubated with appropriate primary Ab for 2 h at room temperature: anti-HA (monoclonal, 1:1,000), anti-GFP (monoclonal, 1:1,000), anti-Flag (monoclonal, 1:1,000), anti-Myc (monoclonal, 1:1,000), anti-GST (monoclonal, 1:5,000), and anti-β-tubulin (polyclonal, 1:5,000), respectively. Next, samples were washed three times with TBST buffer and incubated with a secondary Ab for 1 h at room temperature. After washing three times with TBST buffer again, the nitrocellulose membranes were scanned and imaged using an Odyssey® CLx Imaging System (LICOR Biosciences, USA). The results were obtained from three independent experiments.

Confocal fluorescence microscopy (CFM)

For subcellular localization, co-transfected cells were plated on microscope cover glasses, fixed with 4% formaldehyde for 10 min at 37°C, and incubated with 1 μg/ml Hoechst33342 for 10 min in dark to stain the nuclear. Afterward, stained cells were rinsed with PBS. Images were taken by a high-resolution microscope (NIKON N-SIM, Japan).

QUANTIFICATION AND STATISTICAL ANALYSIS

Statistics

Statistical analyses and presentation graphics were carried out using the SPSS 16.0 and GraphPad Prism 8.0 software, respectively. Results were presented as mean ± SD for at least three independent experiments. All data were subjected to one-way ANOVA, followed by an unpaired, two-tailed t test. p value < 0.05 was considered to be a statistically significant difference (*p < 0.05, **p < 0.01) throughout the manuscript.